UPPSALA
UNIVERSITET

Digital Comprehensive Summaries of Uppsala Dissertations from the Faculty of Science and Technology 1690

Injectable Composite Hydrogels Based on Metal-Ligand Assembly for Biomedical Applications

LIYANG SHI

ACTA
UNIVERSITATIS
UPSALIENSIS
UPPSALA
2018

ISSN 1651-6214
ISBN 978-91-513-0379-6
urn:nbn:se:uu:diva-355252

Dissertation presented at Uppsala University to be publicly examined in Häggsalen, Ångströmlaboratoriet, Lägerhyddsvägen 1, Uppsala, Friday, 14 September 2018 at 13:15 for the degree of Doctor of Philosophy. The examination will be conducted in English. Faculty examiner: Professor Wenxin Wang (University College Dublin (UCD),Charles Institute of Dermatology).

Abstract

Shi, L. 2018. Injectable Composite Hydrogels Based on Metal-Ligand Assembly for Biomedical Applications. *Digital Comprehensive Summaries of Uppsala Dissertations from the Faculty of Science and Technology* 1690. 55 pp. : Acta Universitatis Upsaliensis. ISBN 978-91-513-0379-6.

This thesis presents new strategies to construct injectable hydrogels and their various biomedical applications, such as 3D printing, regenerative medicine and drug delivery. These hydrogels cross-linked by dynamic metal-ligand coordination bonds exhibit shear-thinning and self-healing properties, resulting in the unlimited time window for injection. Compared with non-dynamic networks based on chemically reactive liquid polymer precursors that forms covalent bond during and/or post-injection, our injectable hydrogels with dynamic cross-linkages can be injected from an already cross-linked hydrogel state.

Hyaluronic acid (HA) has been selected as the polymer due to its high biocompatibility and biodegradability. HA has been modified by attaching the bisphosphonates (BP) functionality as ligands for chelation of the metal ions or metal salts to form coordination cross-linkages. In the first part of this thesis, I presented the different chemical approaches to synthesize BP-modified HA (HA-BP) derivatives as well as HA derivatives dually modified with BP and acrylamide (Am) groups (Am-HA-BP). The structures of HA-BP derivatives were confirmed by NMR characterizations, e.g. by the peak at 2.18 ppm for methylene protons adjacent to the bridging carbon of BP in ^{1}H-NMR spectrum and phosphorus peak at 18.27 ppm in ^{31}P-NMR spectrum, respectively. In the next part, the hydrogels were constructed by simple mixing of HA-BP or Am-HA-BP solution with Ca^{2+} ions (**Paper I**), Ag^{+} ions (**Paper II**), calcium phosphonate coated silk microfibers (CaP@mSF) (**Paper III**), and magnesium silicate ($MgSiO_3$) nanoparticles (**Paper IV**). The presented hydrogels exhibited dynamic features determined by reversible nature of coordination networks formed between of BP moieties of HA-BP or Am-HA-BP and metal ions or metal salts on the surface of the inorganic particles. Dynamic properties were characterized by rheological strain sweep experiments and strain-alternating time sweep experiments. Additionally, reversible coordination hydrogels were demonstrated to be further covalently cross-linked by UV light to form a secondary cross-linkage, allowing an increase of the strength and modulus of the hydrogels. In the last part of this thesis, biomedical applications of these hydrogels were presented. Am-HA-BP•Ca^{2+} hydrogel was extruded, using home-made 3D printer, then fixed by UV irradiation to fabricate multi-layered 3D tube-like construct (**Paper I**). In full-thickness skin defects of rat model, HA-BP•Ag^{+} hydrogel accelerated the wound healing process and increased thickness of newly-regenerated epidermal layer (**Paper II**). In the rat cranial critical defect model, double cross-linked Am-HA-BP•CaP@mSF hydrogel induced new bone formation without addition of biological factors and cells (**Paper III**). The anti-cancer drug loaded hydrogel was also prepared by mixing of the drug loaded $MgSiO_3$ nanoparticles with HA-BP solution. The released particles from the hydrogel were shown to be taken up by cancer cells to induce a toxic response (**Paper IV**).

In summary, this thesis presents metal-ligand coordination chemical strategies to build injectable hydrogels with dynamic cross-linking resulting in time-independent injection behavior. These hydrogels open new possibilities for use in biomedical areas.

Keywords: injectable, hydrogel, shear-thinning, self-healing, coordination chemistry, biomedical applications

Liyang Shi, Department of Chemistry - Ångström, Polymer Chemistry, Box 538, Uppsala University, SE-751 21 Uppsala, Sweden.

ISSN 1651-6214
ISBN 978-91-513-0379-6
urn:nbn:se:uu:diva-355252 (http://urn.kb.se/resolve?urn=urn:nbn:se:uu:diva-355252)

To my loved family

献给我爱的家人们

List of Papers

This thesis is based on the following papers, which are referred to in the text by their Roman numerals.

I Shi, L., Carstensen, H., Hölzl, K., Lunzer, M., Li, H., Hilborn, J., Ovsianikov A., Ossipov D. (2017) Dynamic Coordination Chemistry Enables Free Directional Printing of Biopolymer Hydrogel. *Chemistry of Materials*, 29: 5816-5823.

II Shi, L., Zhao, Y., Xie, Q., Fan, C., Hilborn, J., Dai, J., Ossipov, D. (2018) Moldable Hyaluronan Hydrogel Enabled by Dynamic Metal-Bisphosphonate Coordination Chemistry for Wound Healing. *Advanced Healthcare Materials*,7: 1700973.

III Shi, L., Wang, F., Zhu, W., Xu, Z., Fuchs, S., Hilborn J., Zhu, L., Ma, Q., Wang, Y., Weng, X., Ossipov, D. (2017) Self-Healing Silk Fibroin-Based Hydrogel for Bone Regeneration: Dynamic Metal-Ligand Self-Assembly Approach, *Advanced Functional Materials*, 27: 1700591.

IV Shi, L., Han, Y., Hilborn, J., Ossipov, D. (2016) "Smart" drug loaded nanoparticle delivery from a self-healing hydrogel enabled by dynamic magnesium biopolymer chemistry. *Chemical Communications*,52: 11151-11154.

Publications not included in the thesis

I Shi, L., Zhang, Y., Ossipov, D. (2018) Enzymatic degradation of hyaluronan hydrogels with different capacity for in situ biomineralization. *Biopolymers*, 109:e23090.

II Chen, S., Shi, L., Luo, J., Engqvist, H. (2018) Novel Fast-Setting Mineral Trioxide Aggregate: Its Formulation, Chemical-Physical Properties, and Cytocompatibility. *ACS Appl. Mater. Interfaces*, 10: 20334-20341.

III Xu, Z., Shi, L., Hu, D., Hu, B., Yang, M., Zhu, L. (2016) Formation of hierarchical bone-like apatites on silk microfiber templates via biomineralization. *RSC Adv.*, 6: 76426-76433.

IV Yang, X., Shi, L., Guo X.,Gao, J., Ossipov, D. (2016) Convergent in situ assembly of injectable lipogel for enzymatically controlled and targeted delivery of hydrophilic molecules. *Carbohydrate Polymers*, 54: 62-69.

V Xu, Z., Shi, L., Yang M., Zhang H., Zhu L. (2015) Fabrication of a novel blended membrane with chitosan and silk microfibers for wound healing: characterization, in vitro and in vivo. *J. Mater. Chem. B*, 3: 3634-3642.

VI Kheirabadi, M., Shi, L., Bagheri, R., Kabiri, K., Hilborn, J., Ossipov, D. (2015) In situ forming interpenetrating hydrogels of hyaluronic acid hybridized with iron oxide nanoparticles. *Biomaterials science*, 3: 1466-1474.

My contributions to the papers in this thesis

I I contributed to the design of work, performed all syntheses, polymers structure characterizations, hydrogel preparations and characterizations, 3D printing experiments on the surface of glass and in hydrogel bath, participated in the discussion of results and wrote the manuscript.

II I contributed to the design of work, performed all syntheses, polymers structure characterizations, hydrogel preparations and characterizations, participated in the discussion of results and wrote the manuscript.

III I contributed to the design of work, performed all syntheses, polymers structure characterizations, prepared all materials except for CaP@mSF, performed all rheological and SEM characterizations and hydrogel swelling experiments, participated in the discussion of the results and wrote the manuscript.

IV I contributed to the design of work, performed all syntheses, hydrogel preparations and characterizations, all experiments except for TEM observation, participated in the discussion of results and wrote the manuscript.

Contents

1 Introduction 15
1.1 Injectable hydrogels 15
1.2 *In situ* covalently cross-linked injectable hydrogels 15
1.3 Hydrogels with time-independent injection behavior 18
1.3.1 Hydrogels cross-linked via metal-ligand coordination 19
1.3.2 Hydrogels formed by host-guest interactions 20
1.3.3 Hydrogels cross-linked by hydrogen bonds 21
1.3.4 Peptide or protein self-assembled hydrogels 21
1.3.5 Colloidal hydrogels 22
1.4 Considerations for use of coordination chemistry in hydrogel formation 23
1.5 Biopolymers used in this thesis 24
1.5.1 Hyaluronic acid (HA) 24
1.5.2 *Bombyx mori* Silk 25
2 Results and Discussion 27
2.1 Bisphosphonate-functionalized hyaluronic acid (HA-BP) 27
2.1.1 Conjugation strategies 27
2.1.2 Characterization of HA-BP derivatives by NMR 28
2.2 Hyaluronic acid dually functionalized with acrylamide and bisphosphonate groups (Am-HA-BP) 29
2.3 Formation of dynamic HA-BP hydrogels by metal ions 31
2.3.1 HA-BP•Ca^{2+} hydrogel 31
2.3.2 HA-BP•Ag^{+} hydrogel 32
2.4 Hydrogels formed by HA-BP polymers and particles 34
2.4.1 HA-BP•CaP@mSF hydrogel 34
2.4.2 HA-BP•$MgSiO_3$ hydrogel 35
2.5 Doubly cross-linked Am-HA-BP•Me^{n+} hydrogel 36
2.6 Hydrogel bioink for 3D printing 37
2.7 Wound-healing hydrogel 40
2.8 Bone-regenerative scaffold 42
2.9 Drug delivery system 43
3 Concluding remarks and future perspectives 46
3.1 Ongoing studies 47
4 Acknowledgement 48
5 Svensk sammanfattning 50
6 References 52

Abbreviations

3D	Three-dimensional
Ad	Adamantane
Am	Acrylamide
BP	Bisphosphonate
BPs	Bisphosphonates
CAD	Computer-aid design
CaP	Calcium phosphate
CaP@mSF	Calcium phosphate coated silk microfibers
Cat	Catechol
CD	Cyclodextrin
Dox	Doxorubicin
DTT	Dithiothreitol
ECM	Extracellular matrix
EDC	1-ethyl-3-(3-dimethylaminopropyl) carbodiimide
EDTA	Ethylenediaminetetraacetic acid
FDA	Food and Drug Administration
G’	Storage modulus
G”	Loss modulus
GAG	Glycosaminoglycan
HA	Hyaluronic acid
HAS	Hyaluronan synthases
HoBt	Hydroxybenzotriazole
Mal	Maleimide group
MA	Methacrylate
$MgSiO_3$@Dox	Doxorubicin loaded $MgSiO_3$
mSF	Silk microfibers
NPs	Nanoparticles
PVA	Polyvinyl alcohol
PBS	Phosphate buffered saline
PEG	Polyethylene glycol
PEMA	Poly-(ethylene-co-maleic acid)
PLA	Poly(L-lactic acid)
PLGA	Poly-(D,L-lactic-co-glycolic acid)
PVAm	Polyvinylamine
UV	Ultraviolet
UDP	Uridine diphosphate
SH	Thiol group

SSPy	Disulfide pyridyl
UPy	Ureidopyrimidinone

Scope of thesis

This thesis focuses on the design and fabrication of injectable composite hydrogels with dynamic features (i.e., shear-thinning and self-healing properties) as well as applications of those hydrogels in various biomedical fields. To realize smooth injection of hydrogels from a non-flowing gel state, dynamic metal-ligand coordination assembly was applied to form reversible cross-linkages of the networks. Compared with the non-dynamic bonds forming injectable hydrogels based on cross-linking of liquid polymer precursors during or after injection, the dynamic system presented in this thesis exhibited unlimited time window for injection. For biomedical use, shear-thinning and self-healing properties efficiently provides more smooth bioprinting process as well as easier delivery of hydrogels to the body.

In this thesis, we modified hyaluronic acid (HA) with bisphosphonate (BP) as chelating ligand based on three different pathways to obtain BP-functionalized HA (HA-BP) (shown in section **2.1**). To obtain strong mechanical properties for hydrogels, a photo cross-linkable group (i.e, acrylamide (Am)) was introduced into HA-BP backbones to obtain Am-HA-BP derivative (shown section in **2.2**). Additionally, two types of metal ions (i.e., Ca^{2+} (**Paper I**) and Ag^{+} (**Paper II**) ions) as well as two types of metal salts particles (i.e., calcium phosphate coated silk microfibers (CaP@mSF) (**Paper III)** and magnesium silicate ($MgSiO_3$) nanoparticles (**Paper IV**)) were introduced into HA-BP or Am-HA-BP solution to generate dynamic hydrogels based on the reversible coordination cross-linking between BP moieties of HA-BP and metal ions. Additionally, the hydrogels can form a secondary cross-linkage with covalent bonds under UV curing. The presented four types of HA-BP based hydrogels were applied in several biomedical applications such as 3D printing (**Paper I**), wound healing (**Paper II**), bone regeneration (**Paper III**), and controlled anticancer drug delivery (**Paper IV**).

Figure 1.1 summarizes all HA derivatives prepared for this thesis, the hydrogels obtained from these derivatives as well as the biomedical applications for which these materials were tested. This thesis provides facile chemical strategies for constructing injectable hydrogels with time-independent injection property for biomedical applications.

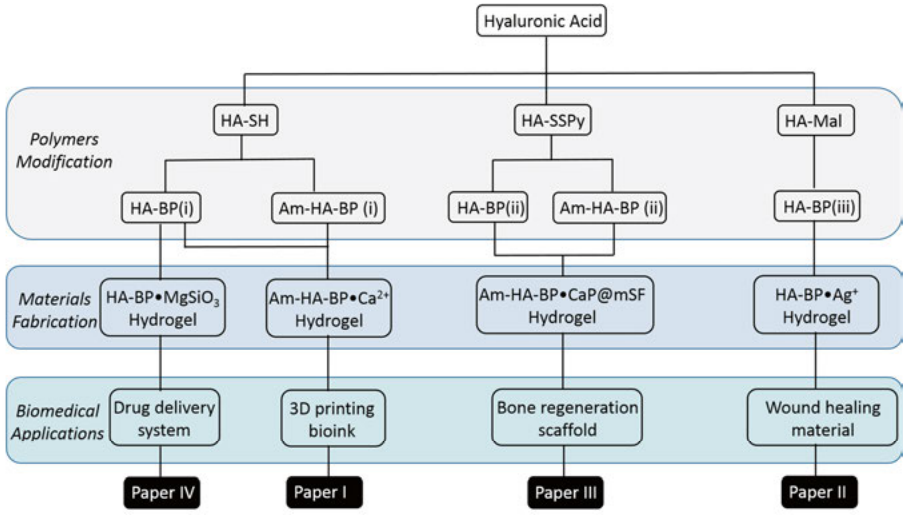

Figure 1.1 Overview of various HA-BP based hydrogels presented in this thesis and biomedical applications for which the hydrogels were utilized. Derivatives HA-BP (i), HA-BP(ii), and HA-BP(iii) represent three different types of attachment of BP moieties to HA backbone.

1 Introduction

1.1 Injectable hydrogels

Hydrogels are three-dimensional (3D) hydrophilic polymeric networks cross-linked by chemical covalent bonds, physical interactions, or the combination of both. Due to the crosslinks between polymer chains and hydrophilic nature of polymers, hydrogels can swell up to hundred or even thousand times their dried mass without being dissolved in a water environment.[1] The structures of hydrogel have similarities with that of extracellular matrix (ECM), allowing its wide use in many biomedical/pharmaceutical areas ranging from drug delivery, 3D bioprinting, biosensor devices to tissue regenerative medicine.[2-5] Hydrogels are generally fabricated either by polymerization of water soluble monomers or cross-linking of polymers.[6] To obtain the hydrogels with biocompatibility to tissues and cells, it is better to exclude the use of toxic monomers and harmful cross-linking reactions during the gelation process. Under mild cross-linking conditions, sensitive molecules including growth factors, therapeutic drugs, and nucleic acid as well as living cells can be encapsulated in hydrogels.[7, 8]

Previously, hydrogels were usaully pre-prepared and implanted into target sites in the body using heavy invasive surgical procedures.[9] In the last three decades, hydrogels that can be injected from a reservoir (e.g. syringe) through a fine needle has gained significant attention in biomedical areas.[9] The injectable hydrogels are high potent in the development of minimally invasive delivery procedures which avoid damage of surrounding tissues during implantation surgery. Injectable hydrogels are also able to fill easily complex-shaped defects *in situ*. Moreover, by automation of hydrogels extrusion from a syringe and programming the extruder movements in computer-aid design (CAD) file, injectable hydrogel can be easily printed out three-dimensionally to fabricate the customized advanced morphology hydrogels.[10]

1.2 *In situ* covalently cross-linked injectable hydrogels

For biomedical applications, the most commonly used approach for injectable hydrogel is *in situ* cross-linking with covalent bonds, where the gelation occurs under physiological conditions upon injection. The covalent bonds can

be formed by various reactions including copper free "click" chemistry, Michael additional reactions, enzymatic reactions, disulfide-forming reactions, UV-light mediated polymerization, etc.[11, 12] The use of non-toxic cross-linkers, no release of harmful side products during cross-linking, and sufficiently rapid gelation kinetics are crucial and need to be considered when developing *in-situ* injectable hydrogels for biomedical applications.

To perform injection of formulation, which undergoes a rapid transition from a liquid to a gel state as the result of chemical reaction, specifically designed double barrel syringes must be used to separate two hydrogel precursors. Upon co-extrusion of the hydrogel precursors (usually aqueous solutions), the polymeric reactants are mixed already in a needle and the mixed polymer solutions is quickly transformed into hydrogel post-injection. Normally, macromolecules of the same or different kinds are modified with mutually reactive groups A and B, respectively, and the "A+B" reaction generates multiple "AB" cross-linkages between all the macromolecules. In this thesis, hydrogels obtained by this method are considered to belong to "A+B"-type systems (Figure 1.2). Our group developed "A+B"-type injectable hydrogels based on thiol-disulfide exchange reaction with fast reaction kinetics at pH 7.0 environment between thiol group installed on hyaluronic acid (HA) molecule and 2-dithiopyridyl groups on another HA molecule.[13] Several other chemical reactions developed by our group or other research groups including thiol-acrylate Michael addition,[14] azide-cyclooctyne copper-free click chemistry,[15] and hydrazone-formation reaction,[16] were applied to design injectable "A+B"-type hydrogels.

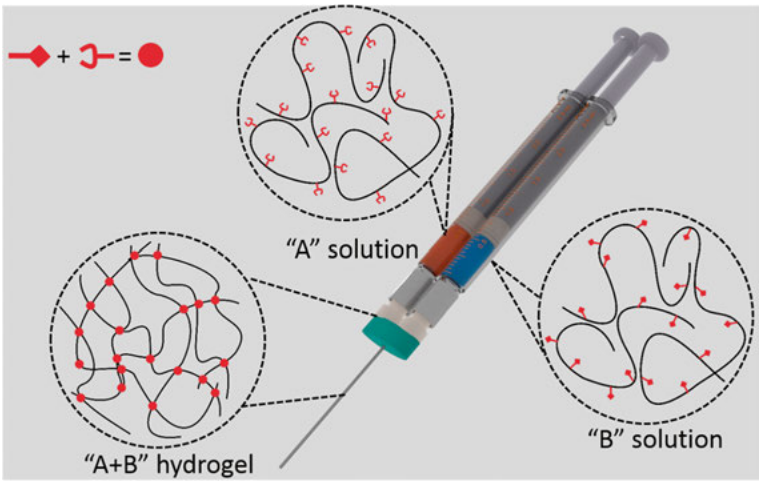

Figure 1.2 Schematic of the injectable "A+B" hydrogels using double barrel syringe, which are cross-linked by covalent bonds during or after injection.

Besides "A+B" systems, another type of injectable hydrogels based on covalent networks are formed from liquid hydrogel precursor under stimuli, for instance, UV-light. Many polymers (e.g. HA,[17] polyethylene glycol (PEG),[18] gelatin[19]) chains have been derivatized with acrylate, methacrylate, or acrylamide groups to obtain water-soluble and photo cross-linkable hydrogel precursors. Upon irradiation with UV or visible light, the photo-initiator is decomposed and free radicals are produced, thus initiating the polymerization reaction and forming irreversibly covalent networks (Figure 1.3).

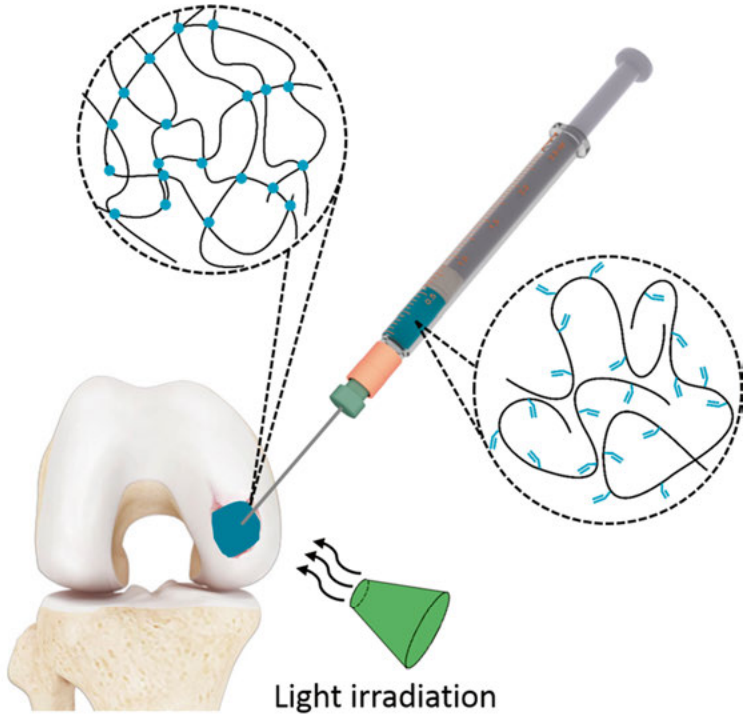

Figure 1.3 The hydrogel precursors consisting of the polymer chain containing UV cross-linkable groups are ejected out from syringe at liquids which is followed by polymerization cross-linked in defect area using light.

The two above categories of covalently cross-linked injectable hydrogels are based on the change from an uncross-linked (liquid) to the cross-linked (network) state. In practice, one should pay attention for the control of gelation kinetics-too slow gelation rates may lead to cargo molecules (drugs) diffusion and loss from the target sites, while too rapid cross-linking may clog needles as well as cause the non-reproducible solidification and rheological properties of the deposited hydrogel. Therefore, the time window for injection is limited, being determined by cross-linking kinetics rates of networks.

1.3 Hydrogels with time-independent injection behavior

The hydrogels based on dynamic cross-linking easily break under shear stress, showing viscosity decrease (i.e., shear-thinning properties).[20] When removing a force (after injection), the dynamic networks are able to recover during a certain short time (i.e., self-healing properties) (Figure 1.4). Shear-thinning properties of a hydrogel guarantees its flow smoothly through a tiny needle. Meanwhile, the hydrogels self-healing properties provide that integrities and mechanical properties of the deposited materials are restored post-injection to the initial level before injection. Due to shear-thinning properties, only a small force is needed to apply to hydrogels during injection, shielding the encapsulated cell and growth factors from a high shear force.

In contrast to non-dynamic cross-linking (usually covalent bonds) based hydrogels that undergo liquid-to-gel transition only once, i.e., during injection or post-injection, hydrogels with dynamic (reversible) cross-linking can exist in gel sate at any time, i.e., even before injection. Assuming that a force is applied only during the injection, a hydrogel with dynamic (i.e., shear-thinning and self-healing) properties behaves as a liquid during injection and is immediately transformed to a gel state after deposition, showing independence from the time of injection. The shear-thinning and self-healing hydrogels can be prepared in advanced (*ex vivo*), can be stored in syringe, and flow through needle whenever it is needed. Therefore, those hydrogels can be easily handled by a surgeon in the clinic.

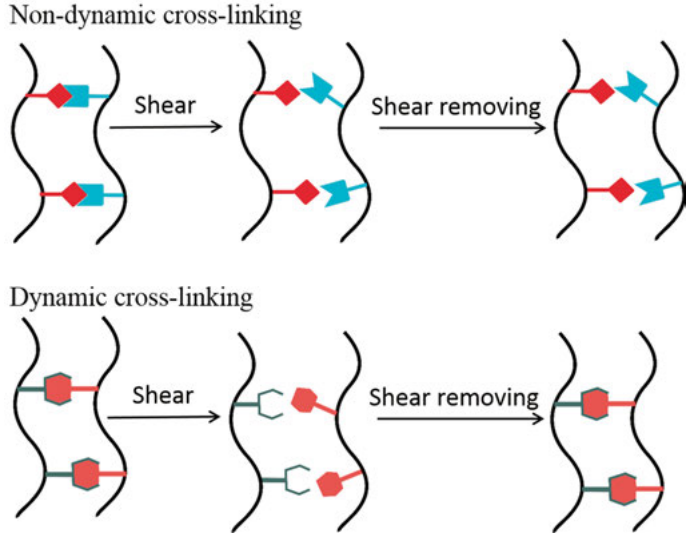

Figure 1.4 Comparison of hydrogels networks with non-dynamic and dynamic cross-linking.

When designing shear-thinning and self-healing hydrogels, equilibrium constant (K_{eq}) of cross-linking as well as kinetics defined as the rate of association (k_a) and disassociation (k_d) are the most important parameters (Figure 1.5). In polymeric networks, it is unequivocal that associated bond represents an "active" cross-linkage, while the disassociated bond represents an "inactive" cross-linkage.[21] The macroscopical hydrogel is only formed above a particular gel point when the number of "active" linkages per volume unit (i.e., cross-linking density) is sufficient to give contiguous networks. Too low K_{eq} value and /or too low concentration of associated linkages concentrations prevent an entire network formation.[21, 22] On the other hand, too large K_{eq} value results in too stable networks to carry "break-after-recovery" dynamic characters.[22] In this case a hydrogel would more resemble as irreversibly cross-linked network.

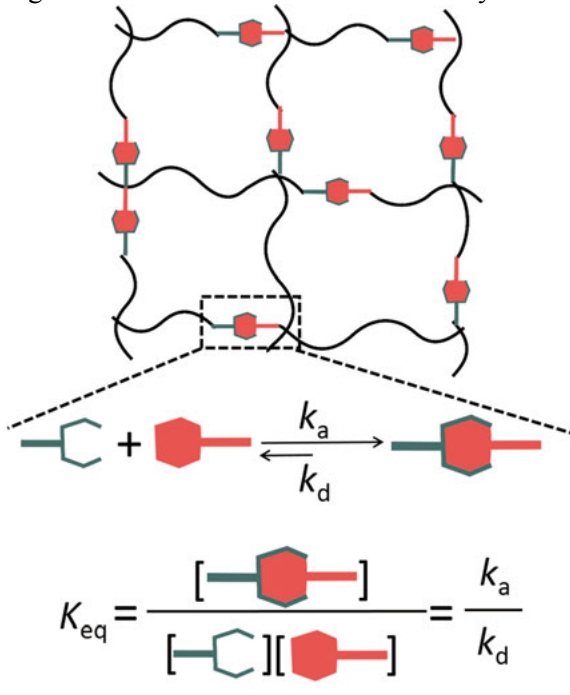

Figure 1.5 Schematic illustration of dynamic network based on reversible cross-linkages. The association of complex formation is expected as a relationship between equilibrium constants (K_{eq}) for cross-linking and association (k_a) and disassociation rates (k_d).

1.3.1 Hydrogels cross-linked via metal-ligand coordination

Coordination bonds between metal ions and organic chelating ligands is a promising strategy for the design of dynamic cross-linkages based injectable hydrogels.[23] In contrast to covalent bonds, coordination bonds are formed as result of donation of an electron pair from a donor ligand to metal ion. Hence, the binding energy for a coordination bond is often lower than the binding

energy for a covalent bond but higher than the binding energy for non-covalent interactions.[24] The most common example of coordination bonds in nature are the bonds in complexes between bis- and tris-catechol and Fe^{3+} ions as found in byssal threads, reported by the Harrington group.[25] Inspired by coordination mechanism, Holten-Andersen and co-workers developed a dynamic hydrogel with self-healing properties based on catechol-functionalized PEG (PEG-Cat) and Fe^{3+} ions.[26] By increasing the pH value of the hydrogel formulation, the cross-linking were changed from monocatechol•Fe^{3+} complexes to bis- and triscatechol• Fe^{3+} complexes. A viscous liquid instead of hydrogel was obtained at pH∼5, whereas the bulk hydrogel was formed at pH ∼ 8 and pH ∼ 12. Besides of free Fe^{3+} ions, iron oxide nanoparticles (Fe_3O_4 NPs) were also able to give a magnetic dynamic hydrogel with PEG-cat solution.[27]

In this thesis, I present another ligand, bisphosphonates (BP), to chelate metal ions and form self-healing and shear-thinning hydrogels. In comparision with catechol system, hydrogels based on BP•Me^{n+} (Me^{n+} is a metal ions) coordination chemistry are formed in physiological environment, thus providing a promising platform for encapsulation of cells and biologically active molecules such as growth factors, etc. Although histidine,[28] carboxylate,[29] and pyridine ligands[30] have also been used for development of dynamic hydrogels with metallic cations, few dynamic hydrogels were exploited in real biomedical applications due to mainly non-physiological conditions required for hydrogel preparation.

1.3.2 Hydrogels formed by host-guest interactions

Host-guest interaction is another type of dynamic interactions that has been widely exploited for dynamic hydrogel preparation. The most popular host molecule used was cyclodextrin (CD) which consists of D-glucopyranoside repeating units linked by the glycosidic linkages into a cyclic structure with an inner hydrophobic cavity. The interior cavity of the macrocycle can host hydrophobic molecules of suitable size. Adamantane (Ad),[31] azobenzene,[32] ferrocene,[33] n-butyl, and t-butyl derivatives [34] have been widely applied as guest. For hydrogel development, guest molecule (CD) and host molecule (Ad) have to be conjugated to the backbones of a hydrophilic polymer. The CD-Ad complex is formed quickly after mixing the above two modified polymer derivatives, leading to the hydrogel formation.[31] Due to the disassociation of CD-Ad complex under an external force, the hydrogel shows shear-thinning properties. On the other hand, the hydrogel network is able to recover immediately and completely when shear stress is removed (self-healing). Another similar method for the development of host-guest hydrogels is based on the formulation of free host molecule (e.g., cucurbit[8]uril) and guest ligands (naphthyl and viologen) functionalized hydrophilic polymers.[35] One cucurbit[8]uril molecules can host both one naphthyl moiety and one viologen moiety thus linking two different polymer chains to which these guest ligands are attached.

Although many advanced studies on injectable hydrogels based on host-guest interactions for biomedical application have been reported, the real use of this system in the clinic has still many practical challenges. For example, it is not yet clear if the various host and guest moieties can induce the long-term toxicity effect, immunological reaction, and biodegradation effect, etc. In-depth investigation of the biological interactions between the supramolecular systems and living tissues or organs have to be exploited before use them in the clinic.[36]

1.3.3 Hydrogels cross-linked by hydrogen bonds

Hydrogen bond is a special type of dipole-dipole interaction, which occurs when a hydrogen atom covalently bonded to a strongly electronegative atom (such as nitrogen (N), oxygen (O), or fluorine (F)) interacts with near-by another electronegative atom with a lone pair of electrons. Generally, hydrogen bonds are stronger than van der Waals interactions, and weaker than covalent bonds, whose bonding strength always stands between 4 and 120 kJ mol^{-1}.[37,38] Despite of the weakness of a single hydrogen bond, multiple hydrogen bonds can contribute significantly to the overall "active" cross-linkages and result in the formation of a bulk injectable hydrogel.

Dankers group conjugated ureidopyrimidinone (UPy) group to PEG chain via alkyl-urea spacers. In this system, the interaction of UPy-UPy is shielded from the aqueous environment within the hydrophobic pocket based on the alkyl spacers. 1D fibers are self-assembled due to UPy dimerization by hydrogen bonding. The injectable UPy hydrogel is further obtained by assembly and entanglement of the 1D fibers. Due to the inherent dynamic properties of UPy-UPy interaction, this hydrogel exhibits shear-thinning and self-healing properties, thus making it easy for valuable delivery to a pig myocardial infarction heart by catheter-mediated injection.[39, 40]

1.3.4 Peptide or protein self-assembled hydrogels

Self-assembling of peptides or proteins is another promising approach in the formation of supramolecular hydrogel with thixotropic properties. In this system, the dynamic cross-linkages are always formed based on a combination of multiple types of non-covalent bonds such as hydrogen bonding, hydrophobic interactions and electrostatic interactions. For example, Pochan and Schneider group developed a family of injectable self-assembled hydrogels based on β-hairpin peptides, namely "MAX" sequence. The well-known MAX1 peptide consists of two strands of alternating lysine and valine residues conjugated by a Val^{D}-Pro-Pro-Tyr type II' β-turn linker. The typical sequence of MAX1 is H_2N-$(Val\text{-}Lys)_4$-Val^{D}-Pro-Pro-Tyr-$(Val\text{-}Lys)_4$-$CONH_2$. In this system, the β-hairpin structure is folded due to the intermolecular interactions when the charge repulsion between neighboring Lys residues is decreased by

increasing the pH value of the formulation or by ionic shielding with exogenous salt. The long fibers (200 nm) are grown based on hairpin pairs driven by forces of hydrogen bonding and hydrophobic interactions. Furtherly, the hydrogel is formed by non-covalent cross-linkages of interfibril junctions, which is applied as injectable cell and drug vehicle due to its self-healing and shear-thinning properties.[41-43]

Another self-assembled hydrogel was cross-linked as a result of the protein-protein molecular recognition. The group of Heilshorn developed a facile injectable hydrogel with shear-thinning properties by mixing two recombinant protein components containing repetitive WW domain and proline-rich peptide. The WW domain is a modular protein domain, consisting of 20-50 amino acids, with two conserved tryptophans (W), which specifically associates with the proline-rich sequence. The two hydrogel precursors were mixed and the random cross-linkages were formed resulting in the sol-gel transition. This hydrogel showed biocompatibility to various types of cells including human umbilical vein endothelial cells (HUVEC), murine adult neural stem cells (NSCs), PC-12 neuronal-like cells, and adipose-derived stem cells (ASCs). [44-46]

1.3.5 Colloidal hydrogels

Colloidal hydrogel formed by oppositely-charged poly-(D,L-lactic-co-glycolic acid) (PLGA) nanoparticles exhibited shear-thinning properties, which was used as an injectable tissue engineering material and a drug delivery systems. Poly-(ethylene-co-maleic acid) (PEMA) and polyvinylamine (PVAm) were blended into PLGA, to generate the negative and positive charged PLGA NPs, respectively. In this system, the hydrogel was self-assembled by electrostatic forces resulting in the shear-thinning networks which can be broken under the shear force due to the interruption of particle interactions.[47, 48] Besides of synthetic polymers, biopolymers such as gelatin was also used to build particulate-based hydrogel by attractive electrostatic interaction.[49, 50]

1.4 Considerations for use of coordination chemistry in hydrogel formation

Coordination chemistry plays important roles in biological systems such as providing structural and storage integrity, catalytic centers for the metalloproteins or enzymes, as well as providing structural supports for such tissues as human bone, spider teeth, and insect mandible.[51,52] In biomaterials application, metal-ligand cross-linking offers several advantages in achieving materials with specific properties: 1) equilibrium constants (K_{eq}) for metal-ligand bonds stands in a very broad window from 10^3 to 10^{40}, depending on the types of ligand and metal cation (Figure 1.6). Therefore, metal-ligand chemistry is able to provide various strength cross-linkages to form both soft and hard materials. 2) Many metal-ligand bonds are inherently reversible, resulting in the hydrogels with self-healing and shear-thinning properties. 3) Metal-ligand bonds can be cleaved or formed by pH change, a feature exploited in formation of pH-sensitive biomaterials for drug delivery applications.[53]

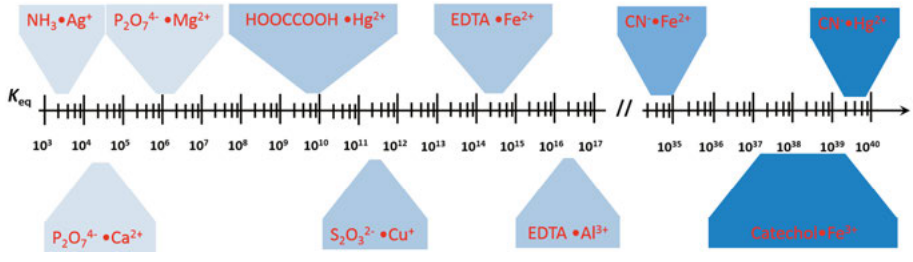

Figure 1.6 Schematics showing the range of K_{eq} values for metal-ligand coordination bonds formed between different types of ligands and metal ions.

Bisphosphonates (BPs) is a very well-known family of drugs to treat the calcium loss diseases, such as osteoporosis, which were introduced half-century ago. BPs are chemically stable synthetic analogues of pyrophosphate, in which the oxygen-bridged P-O-P structure is replaced by carbon atom containing P-C-P structure (Figure 1.7), resulting in the resistance to hydrolysis, common for pyrophosphate.[54] Based on the R1 and R2 substituent groups, BP are grouped into two main classes of compounds, non-nitrogen bisphosphonates (NN-BPs) and nitrogen bisphosphonates (N-BPs) (Figure 1.7). As many studies showed, BPs exhibit great affinity to both metal ions (i.e., Ca^{2+} ions) and minerals (i.e., hydroxyapatite) through coordination chemistry.[55] However, the binding forces with metal ions differ by the changing of the R1 and R2 groups. For example, if R1= hydroxyl group (OH), the corresponding BPs are able to provide more stable tridentate binding to Ca^{2+}, while such R1 groups as Cl and H result in much weaker affinity to metal cations.[55]

In my thesis, pamidronate was selected as a chelating ligand to functionalize the HA backbones. Pamidronate forms differently protonated mononuclear

and dimeric complexes with Ca^{2+} cations once coordinated in aqueous solution. At low pH (around 6.0), the complexes of Ca^{2+} ions with pamidronate exist as H_2L•Ca, followed by HL•Ca and L•Ca_2 species with the increase of pH value. Further, the bis-complexes L_2•Ca are formed at pH above 10.[56] Besides of Ca^{2+} ions, many other metal ions including Mg^{2+}, Zn^{2+}, Ag^{+}, Sr^{2+} are also coordinated by pamidronate.[56] In all structures of BP•Me^{n+} complexes, oxygen atoms of phosphonic acid bind the cations. Four decades after the first applications of BP as medical drugs, BP were also widely used as "bone hooks" to deliver other therapeutic compounds and/or imaging agents to target bone via conjugation of BPs to the drugs or imaging agents.[57]

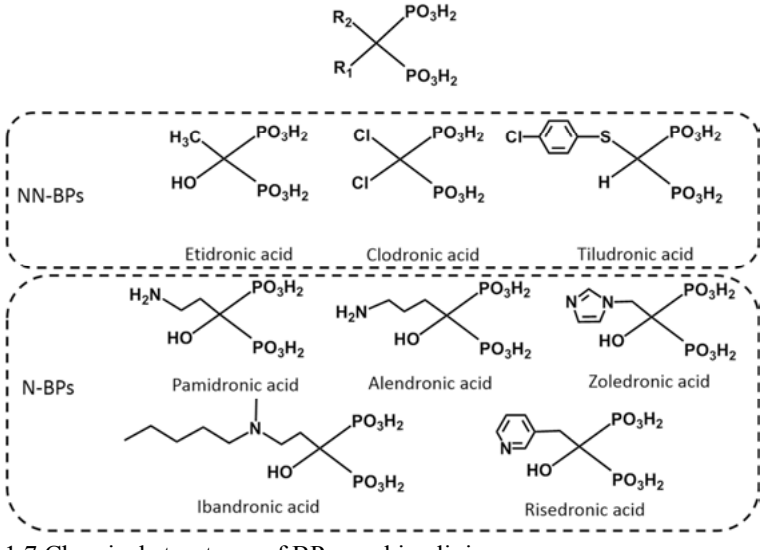

Figure 1.7 Chemical structures of BPs used in clinic.

1.5 Biopolymers used in this thesis

1.5.1 Hyaluronic acid (HA)

HA, also known as hyaluronan, is one of the most important polysaccharides that exists in synovial fluid and in extracellular matrix (ECM) of many human tissues including epithelial, connective, and neural tissues. HA is comprised of repeating disaccharide units of D-glucuronic acid and N-acetyl-D-glucosamine (Figure 1.8), and exhibits the same chain structure independent of species. HA is produced by a family of membrane-bound enzyme, hyaluronan synthases (HAS), on the cell surface by using two substrates, uridine diphosphate (UDP)-α-N-acetyl-D-glucosamine and UDP-α-D-glucuronate, and is secreted across cellular membrane into the ECM space. In 1894, a "mucin" presumably consisting of hyaluronan and protein was isolated from the vitreous in Uppsala by Carl Thore Mörner.[58] In 1934, Karl Meyer and John Palmer

isolated a polysaccharide from the vitreous humor that contained uronic acid and amino sugar and named it as “hyaluronic acid” from hyaloid (vitreous) + uronic acid.[59] The term of “hyaluronan” was introduced to satisfy polysaccharide nomenclature in 1986.[60] In the 1970s, Dr. Endre Balazs developed a facile method for extraction of highly purified and non-inflammatory high molecular weight HA from the umbilical cords and rooster combs, opening the door to several medical applications of HA.[61] Now HA is always produced using the cost-effective and environment-friendly method, e.g., by microbial fermentation.[60]

HA is the only non-sulfated glycosaminoglycan (GAG) in the body and that plays important roles in many biological processes such as wound healing, tissue lubrication, cellular proliferation and morphogenesis, cell motility, embryonic development, cancer metastasis, etc.[62-64] HA has been widely used to build biomaterials for tissue engineering, drug delivery and viscosupplementation. To reduce the rate of degradation *in vivo*, chemical and/or physical methods were applied to cross-link HA. For example, our group developed both chemical and physical strategies for fabrication of cross-linked HA hydrogels, including Schiff-base hydrazone coupling reaction, disulfide cross-linking by thiol-disulfide exchange reaction, and photo-mediated cross-linking of acrylamide-modified HA (**Paper I and III**), as well as metal-ligand coordination (**Paper I, II, III and IV**).

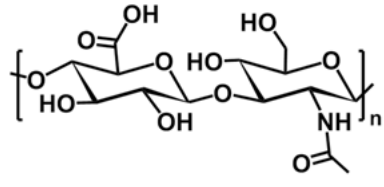

Figure 1.8 Structure of hyaluronic acid

1.5.2 *Bombyx mori* Silk

Silk, extracted from *Bombyx mori* cocoon, is a very promising and widely investigated biopolymer for biomedical applications.[65, 66] Due to the unique features such as high mechanical properties and great biocompatibilities, silk has been used as sutures for centuries. Native silkworm silk consists of silk fibroin and sericin proteins with the adhesive feature, in which silk fibroin is coated and sticked with sericin. By the weight ratio, silk fibroin accounts for 70–80% of silk and sericin accounts for the rest 20–30%. From a molecular perspective, silk fibroin is composed of heavy chain (MW ~390 kDa) and light chain (MW~26 kDa), and they are conjugated together with a disulfide bond.[67] Silk fibroin consists of rich hydrophobic antiparallel β-sheet structures linked by small hydrophilic linker spaces. The β-sheet domain is primarily composed of the repetitive amino acid sequence, Gly-Ala-Gly-Ala-Gly-Ser (GAGAGS), which contributes to the high tensile strength and toughness of silk material.

For instance, silk from *Bombyx mori* possesses much higher ultimate tensile strength value (740 MPa)[68] compared with that for the commonly used biodegradable polymers, e.g., collagen (0.9-7.4 MPa)[69] and poly(L-lactic acid) (PLA) (28-50 MPa)[70]. Many forms of silk fibroin- and sericin-based materials including sponges, hydrogels, films, electrospun nanofibers, are widely explored and fabricated serving as tissue engineering scaffolds, biosensor, "bio-ink" ect.[68, 71, 72] Additionally, easy combination of silk materials with other inorganic and/or organic materials afford an accomplished toolbox for various biomedical applications.

2 Results and Discussion

2.1 Bisphosphonate-functionalized hyaluronic acid (HA-BP)

2.1.1 Conjugation strategies

For functionalization of HA with BP group, several conjugation strategies (Figure 2.1) were used in this thesis including UV-light mediated thiol-ene addition reaction (**Paper I** and **Paper IV**), thiol-disulfide exchange reaction (**Paper III**) and "click"-type Michael addition (**Paper II**). Firstly, three different HA derivatives including thiolated HA (HA-SH), 2-dithiopyridyl modified HA (HA-SSPy), and maleimide (Mal) modified HA (HA-Mal), respectively, were synthesized using 1-ethyl-3-(3-dimethylaminopropyl)carbodiimide (EDC) coupling reaction. Secondly, three HA-BP derivatives with slightly different structures (i.e., HA-BP(i), HA-BP(ii), and HA-BP(iii)) were obtained from HA-SH, HA-SSPy and HA-Mal derivatives, respectively, based on above mentioned three reactions (Figure 2.1). Particularly, the radical thiol-ene addition of acrylamide-modified BP (**2**) to HA-SH lead to a brush-like structure consisting of few BPs moieties per thiol group installed on HA backbone. On the other hand, one BP moiety was only attached one dithiopyridyl or one maleimide group on HA backbones using chemoselective "click"-type conjugation of a thiol-functionalized bisphosphonate (**4**) to HA-SSPy or HA-Mal derivative (Figure 2.1).

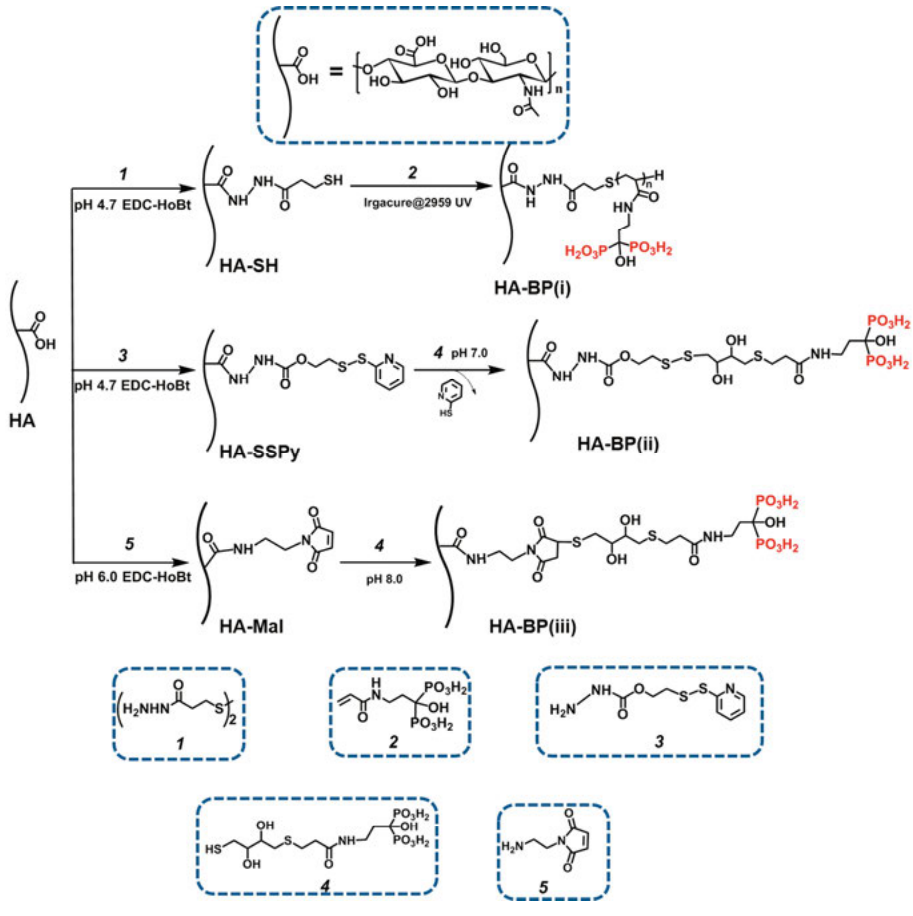

Figure 2.1 Schematic for the syntheses of HA-BP derivatives by three pathways.

2.1.2 Characterization of HA-BP derivatives by NMR

^{1}H-and ^{31}P-NMR spectrometry was used to confirm the structures of three HA-BP derivatives. Particularly, the structure of HA-BP (i) derivative was confirmed by the appearance of a new peak at 2.18 ppm, corresponding to methylene protons, adjacent to the bridging carbon of BP (-$\underline{CH_2}C(OH)(PO_3H_2)_2$) (Figure 2.2a). The BP modification density was found to be around 25%, which was determined by the integration of this peak and comparing with with the integral for acetamide moiety peak at 1.9 ppm. Moreover, the appearance of phosphorus signal at 18.27 ppm in the ^{31}P-NMR spectrum was further confirmed the successful grafting of BP to HA backbone (Figure 2.2b). Similarly, the appearance of new peak at 2.18 ppm (-$\underline{CH_2}C(OH)(PO_3H_2)_2$) and the disappearance of peaks at 7.45, 7.92, 8.06, and 8.45 ppm were characterized as nucleophilic substitution of dithiopyridyl

leaving group leading to the sucessful grafting of BP via disulfide bond which confirmed the successful synthesis of the HA-BP(ii) polymer (Figure 2.2c). Moreover, the peaks in the range between 2.5 and 3.2 ppm were assigned to the ten methylene protons of the linker between BP and HA backbone (-OCH_2CH_2S-$SCH_2CH(OH)CH(OH)CH_2SCH_2CH_2C(O)NH$-). In ^{31}P-NMR spectrum, the same phosphorus signal at 18.27 ppm was also observed for HA-BP(ii) derivative.

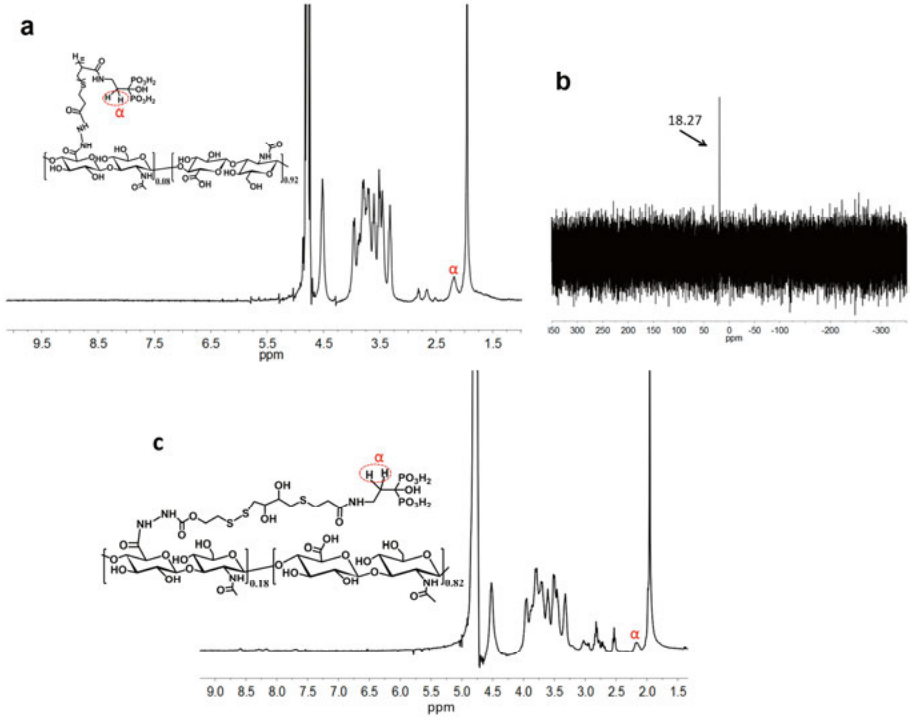

Figure 2.2 ^{1}H-and ^{31}P-NMR spectra of HA-BP derivatives.

2.2 Hyaluronic acid dually functionalized with acrylamide and bisphosphonate groups (Am-HA-BP)

To improve mechanical properties of cooridantion netwroks by additional covalent cross-linking, UV-light polymerizable groups such as acrylamide (Am) should be introduced to HA-BP derivatives. Therefore, we prepared HA derivatives dually functionalized HA with acrylamide and bisphosphonate groups (i.e., Am-HA-BP). One approach to Am-HA-BP derivative is to conjugate Am group on the HA-BP(i) backbone directly by EDC-mediated amidation with reagent **6** (Figure 2.3a). Another method is to graft firstly the Am groups on the backbones of native HA to obtain HA-Am polymer and then to

further functionalize HA-Am with 2-dithiopyridyl (Figure 2.3b). Conjugation of BP groups to Am-HA-SSPy derivative is finally accomplished by thiol-disulfide exchange using reagent **4**, which give Am-HA-BP (ii) (Figure 2.3b). ^{1}H-NMR characterization of the resulting Am-HA-BP(ii) derivative revealed both the peak at 2.18 ppm for the methylene protons linked to the bridging carbon of BP (-$\underline{CH_2}$C(OH)(PO_3H_2)$_2$) and the peaks at 5.7 and 6.2 ppm for Am group (Figure 2.3c). Based on the integration of acetamide moiety of *N*-acetyl-D-glucosamine of HA, degrees of modifications of HA with Am and BP groups were calculated to be ~20% and ~17%, respectively. In comparison with the high Am modification density (~20%) in Am-HA-BP(ii), the maximal amount of Am group in the Am-HA-BP(i) derivative was around 10%, which could be caused by inhibition effect of the phosphonate group on coupling reaction with HA carboxylates. For the synthesis of Am-HA-BP(ii) process, the relatively rapid rate for thiol-disulfide exchange reaction between a thiol groups of reagent **4** and 2-dithiopyridyl of Am-HA-SSPy avoids the risk of a thiol-ene addition of reagent **4** to Am group of Am-HA-SSPy polymer.

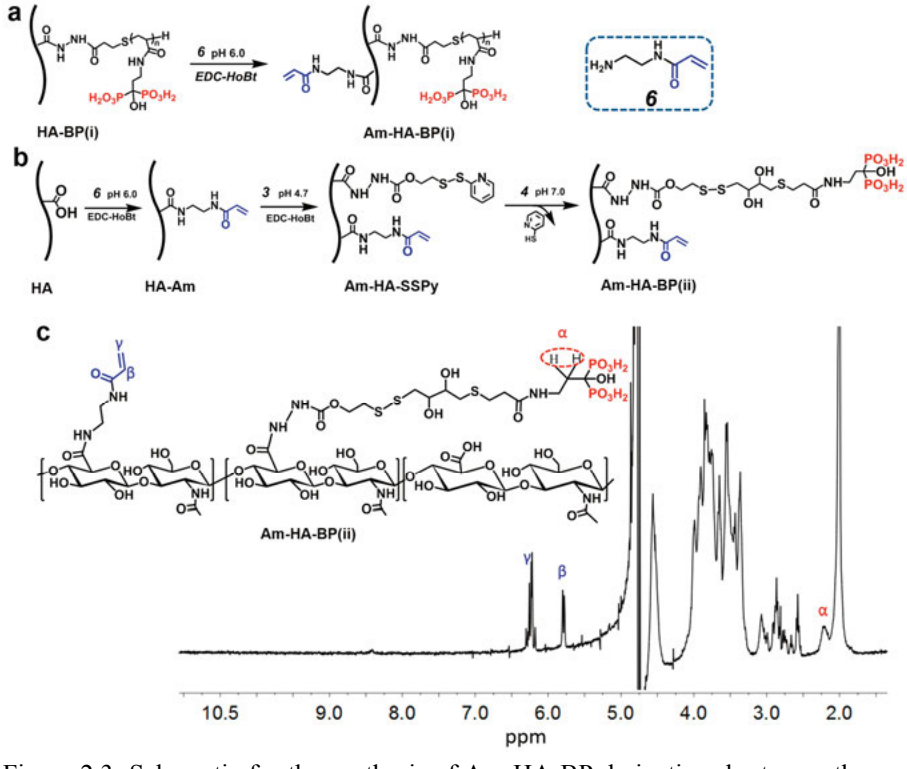

Figure 2.3 Schematic for the synthesis of Am-HA-BP derivatives by two pathways (a,b). ^{1}H-NMR spectrum of Am-HA-BP derivative obtained by second reaction pathway (c). Reagent 3 and 4 are the same compounds as in Figure 2.1.

2.3 Formation of dynamic HA-BP hydrogels by metal ions

2.3.1 HA-BP•Ca^{2+} hydrogel

In **Paper I**, a hydrogel was formed immediately after mixing of HA−BP(i) derivative and a calcium chloride ($CaCl_2$) solution, as a result of cross-linking by coordination complexation of P-O^- groups of BP moieties and Ca^{2+} ions (Figure 2.4a). Additionally, the formation of HA-BP•Ca^{2+} hydrogel was found to depend on the concentrations of two hydrogel precursors, i.e. HA-BP(i) macromolecules and Ca^{2+} cations. As expected, higher concentrations of the precursors aided hydrogel formation (Figure 2.4b). The HA-BP•Ca^{2+} hydrogel (2.7% w/v HA-BP and 200 mM $CaCl_2$) formation was confirmed by the significantly higher storage modulus (G'≈200 Pa) than its loss modulus (G" ≈20 Pa) using rheology frequency sweep measurements between 0.1 to 10 Hz at a fixed strain (1%) (Figure 2.4c). The presented hydrogel showed self-healing feature characterized by the rejoining of the two cut hydrogel pieces (Figure 2.4d). Moreover, the self-healing behavior was also proved by rheology tests, demonstrating immediate and almost complete recovery of G' value upon strain decreasing from high values (400%) to low (1%) value (Figure 2.4e). Based on the data from rheology strain sweep experiment, the hydrogel was elastic with G' > G" at low strain, while it was converted to a highly viscous liquid (i.e., G' < G") at strain above 120% (Figure 2.4f). This shear-thinning property of HA-BP•Ca^{2+} gel allows gliding and time-independent injection of the material from a syringe reservoir. The self-healing property guarantees the hydrogel networks integrity and recoverable mechanical properties after injection.

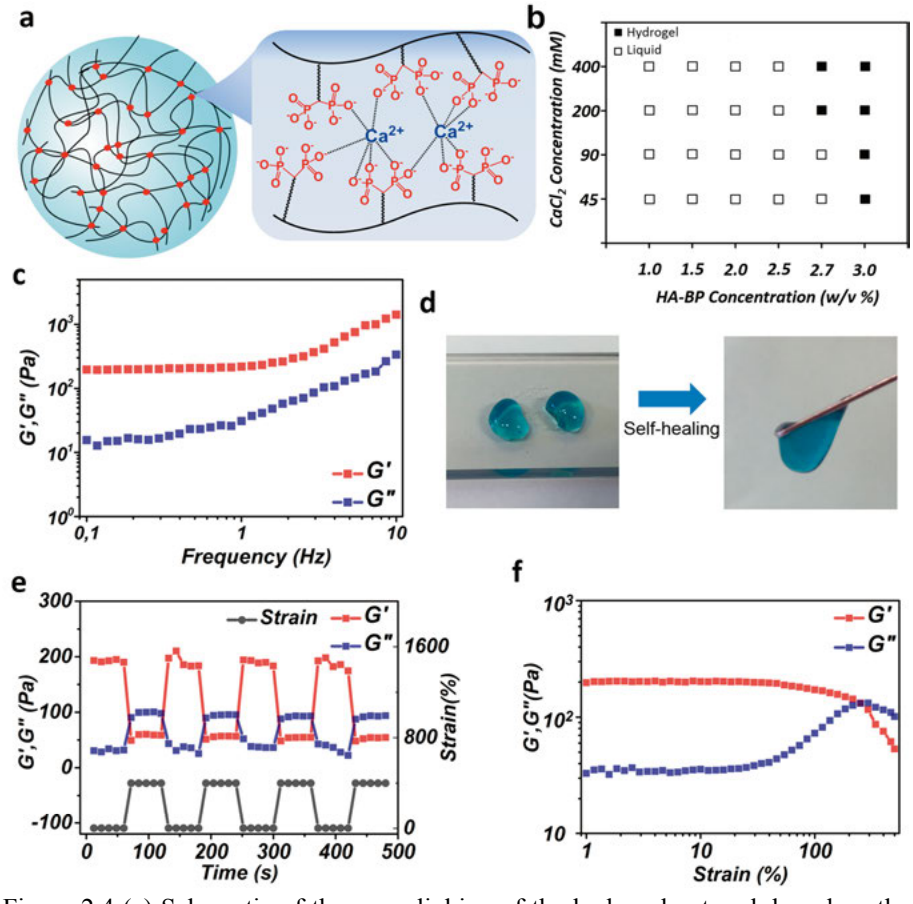

Figure 2.4 (a) Schematic of the cross-linking of the hydrogel network based on the coordination interaction between HA-BP molecules and Ca^{2+} ions. (b) The HA-BP•Ca^{2+} hydrogel formation depends on the concentration of polymers and metal ions. (c) Storage modulus (G') and loss modulus (G") of HA-BP•Ca^{2+} hydrogel. (d) Re-joining of two cut pieces of HA-BP•Ca^{2+} together exhibits the macroscopically self-healing properties. Alcian blue as a dye is dissolved in the hydrogel for visualization. (e) Storage modulus (G') is recovered immediately and completely after the force removal. (f) Shear-thinning properties are demonstrated by the lower storage modulus (G') than loss modulus (G") under stress (i.e., during injection).

2.3.2 HA-BP•Ag^{+} hydrogel

In **Paper II**, the supramolecular HA-BP•Ag^{+} hydrogel (3% w/v HA-BP and 15 mM Ag^{+} ions) was formed almost instantaneously (in few seconds) after mixing of HA-BP(iii) solution with silver nitrate ($AgNO_3$) solutions (Figure 2.5a). To verify if the hydrogel was cross-linked by the coordination bonds between Ag^{+} ions and BP groups on the backbones of HA-BP derivative, the control experiments were performed by mixing $AgNO_3$ solution with native

HA and HA-BP precursor (HA-Mal). The results showed no hydrogel formation for HA or HA-Mal polymers. Further, the interactions between HA-BP(iii) polymers and Ag^+ ions in aqueous phase were studied by UV-vis spectroscopy (Figure 2.5b). Native HA solution, $AgNO_3$ solution, and a mixture of native HA with $AgNO_3$ did not show absorption in the UV region above 300 nm. On the other hand, the band at 304 nm resulted from electron transitions of phosphonate group was observed in the spectrum of HA-BP(iii) solution. The intensity of absorption of pure HA-BP(iii) polymer was 0.178 units at 304 nm, and that was increased five times after introducing Ag^+ ions, namely, A304 nm (HA-BP + Ag^+) = 0.864 units. Red-shifted tail of the band might be induced by the decreased energy of the mixture after coordination with metal ions. The absorption of HA-BP+Ag^+ mixture decreased with the decrease of pH value to 3.5, which proved the fact that protonation of BP groups is able to weaken coordination bonds with metal ions. Due to the dynamic properties of BP•Ag^+ coordination bonds, one piece of HA-BP•Ag^+ supramolecular hydrogel could be molded into different shapes (Figure 2.5c). The cut HA-BP•Ag^+ hydrogel pieces healed together in 30 s using light microscope observation. Rheological tests revealed that the healed hydrogel had the same storage modulus (≈400 Pa) as the hydrogel before damage.

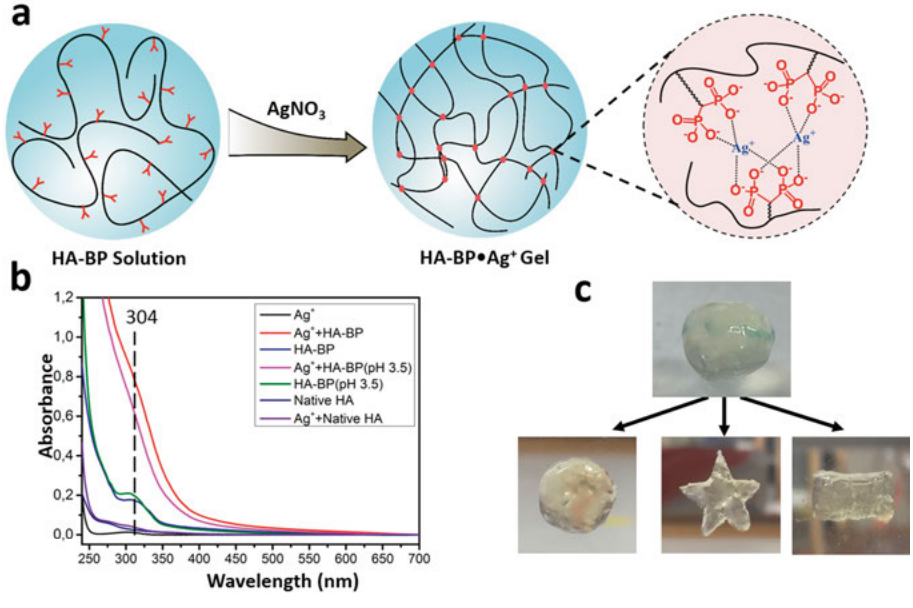

Figure 2.5 (a) Schematic of hydrogel formation based on Ag^+ ions and HA-BP solution. Coordination bonds between BP moieties of HA and Ag^+ ions provide the cross-linking of HA. (b) The UV-vis absorption of native HA, HA-BP, $AgNO_3$ solution, and mixed formulations composed of different HAs and Ag^+ ions. Concentrations of HA and HA-BP polymer was both 3 mg/mL. Ag^+ ions were 1.5×10^{-3} M, corresponding to 1:1 of BP:Ag^+ molar ratio. (c) Supramolecular HA-BP•Ag^+ hydrogel was able to mold into various shapes.

2.4 Hydrogels formed by HA-BP polymers and particles

2.4.1 HA-BP•CaP@mSF hydrogel

To mimic bone structure with unique hierarchical composition based on proteins, minerals and polysaccharides, we developed an injectable hydrogel formed by mixing HA-BP derivative and calcium phosphate (CaP)-coated silk microfibers (mSF) (**paper III)** (Figure 2.6). The hydrogel networks are cross-linked by coordination bonds between $–PO_3^{2-}$ group on the backbone of HA-BP and calcium ions with unoccupied orbitals on the surface of CaP particle of CaP@mSF. The HA-BP•CaP@mSF composite hydrogel (4% w/v CaP@mSF and 2% w/v HA-BP) was able to form rapidly upon mixing of the above two hydrogel precursors under physiologic conditions without any stimuli. Based on the reversibility of BP•CaP coordination bonds, the presented silk-based hydrogel exhibited such dynamic features as shear-thinning and self-healing properties, allowing its time-independent injection behavior. Our hydrogel can be prepared in advance, which enables storage inside a syringe and keeps the structural integrity after injection. Therefore, it is convenient for practical clinical use since surgeons do not need to mix the hydrogel precursors during operation.

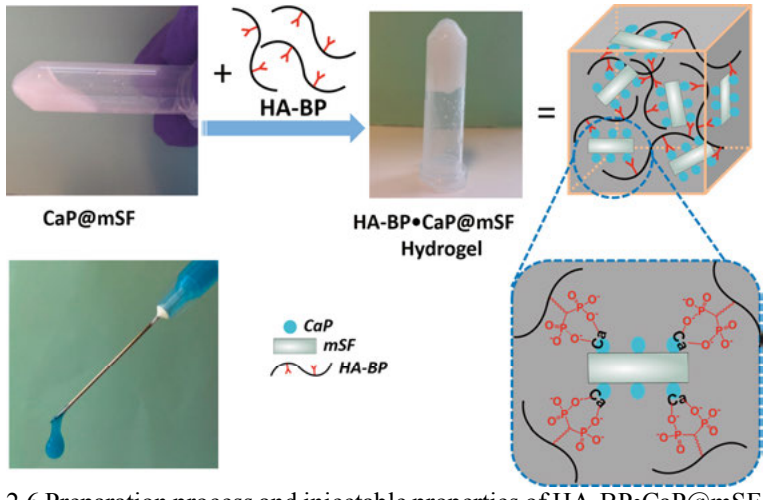

Figure 2.6 Preparation process and injectable properties of HA-BP•CaP@mSF hydrogel. The hydrogel is formed by addition HA-BP polymer binder to CaP@mSF dispersion, and cross-linking by the coordination bonds of BP groups on HA backbones and CaP on the microfibers. For visualization, alcian blue as a dye was dissolved in the hydrogel.

2.4.2 HA-BP•$MgSiO_3$ hydrogel

In **paper IV**, magnesium (Mg) containing NPs, $MgSiO_3$ NPs (size: ~250-~350nm), were introduced to the HA-BP solution to give a composite hydrogel based on coordination cross-linkages of BP ligands of HA-BP polymers and Mg^{2+} ions on $MgSiO_3$ NPs. The quite low solubility of $MgSiO_3$ excludes the possibility of HA-BP•$MgSiO_3$ hydrogel formation by the interaction of BP groups with solvated Mg^{2+} cations. According to coordination number of Mg^{2+}, coordination sphere of magnesium ions in the bulk of the material is fully coordinated with SiO_3^{2-} anions. On the other hand, on the surface of $MgSiO_3$ NPs, metal centres are always not entirely occupied with anions, allowing the vacant valences to be coordinated by other ligands if they are present in the system (or water molecules if there are no other ligands). Therefore, BP ligands of HA-BP should strongly bind to the surface of $MgSiO_3$ NPs.

Rheological experiments based on a time sweep were performed to investigate the kinetics of hydrogel formation (Figure 2.7). $MgSiO_3$ NPs suspension and polymeric HA-BP solution were mixed at 6% and 2% (w/v) of final concentrations, respectively. The rheological tests started to acquire the data 25 min later after mixing. The liquid-to-gel transition indicated by storage modulus (G') > loss modulus (G") was found in the course of around 600 seconds after measuring. Therefore, the total gelation time was around 35 min (together with 25 min waiting time) (Figure 2.7a). However, no gel formations were observed in two control formulations: 1) a mixture of SiO_2 NPs + HA-BP (Figure 2.7 b) and 2) a mixture of $MgSiO_3$ NP + native HA (Figure 2.7c). Therefore, rheological data certainly illustrate the two key factors, BP moieties and Mg^{2+} ions, are crucial for the hydrogel formation. Thanks to the dynamic coordination BP•Mg^{2+} cross-linkages, the HA-BP•$MgSiO_3$ hydrogel also demonstrated shear-thinning and self-healing of reversible properties.

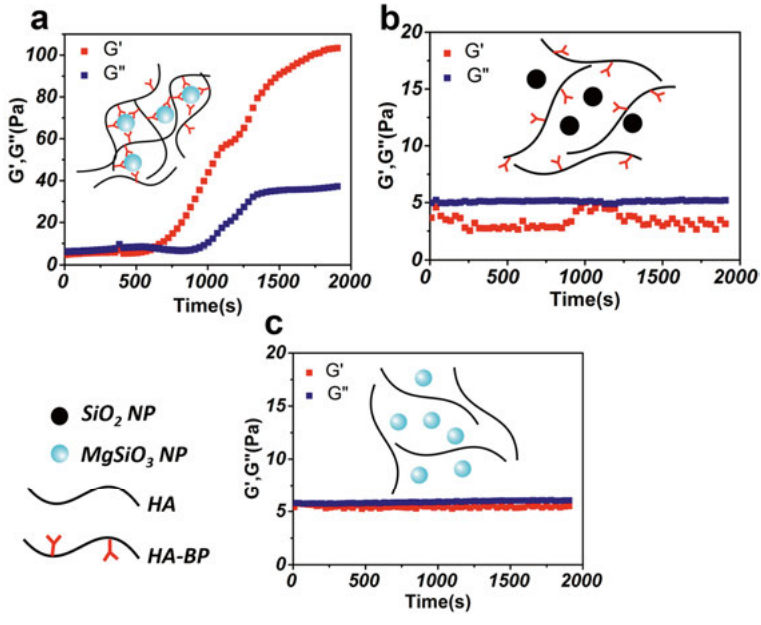

Figure 2.7 (a) The HA-BP•$MgSiO_3$ hydrogel formation was characterized by storage modulus (G') > loss modulus (G") based on rheological kinetics experiments. Control rheological experiments were performed with (b) a mixture of HA-BP polymers + SiO_2 NPs, and (c) a mixture of native HA polymers + $MgSiO_3$ NPs.

2.5 Doubly cross-linked Am-HA-BP•Me^{n+} hydrogel

We found that the hydrogels cross-linked by only coordination bonds between BP ligands and metal ions or metal-containing particles exhibited poor mechanical properties and deficient structural stability under physiological environment. Therefore, both Am and BP moieties were simultaneously introduced into HA backbone to obtain dually functionalized Am-HA-BP derivative (shown as Figure 2.2), which is able to form another covalent cross-linking based on photo-mediate radical reaction (Figure 2.8a). In the Am-HA-BP•CaP@mSF hydrogel system, the G' values are increased 10-fold from ≈250 Pa to ≈2.5 kPa after 10 min of UV illumination (Figure 2.8b). The hydrogel only cross-linked by coordination BP•CaP bonds (i.e., pre-UV exposure) is gradually dissolved in 5 hours of incubation in phosphate buffered saline (PBS). On the other hand, swelling ratio of Am-HA-BP•CaP@mSF hydrogel doubly cross-linked by both coordination interactions and covalent bonds (i.e., post-UV exposure) displays only a small increase (≈20%) even after 72 hours of incubation, demonstrating its excellent structural stability.

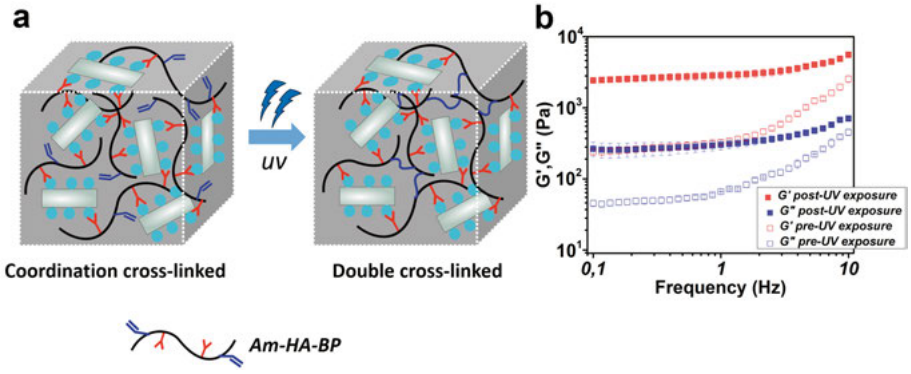

Figure 2.8 (a) Schematics of coordination network and the formation of second covalent cross-linking after UV exposure of Am-HA-BP•CaP@mSF hydrogel for 10 min. (b) Comparison of mechanical properties of Am-HA-BP•CaP@mSF hydrogel before and after photo-crosslinking.

2.6 Hydrogel bioink for 3D printing

3D printing technology is a promising approach to fabricate customized biomaterials. Various hydrogels based on biopolymers or/and synthetic polymers, such as alginate,[73] pluronics,[74] and gelatin,[75] have been applied as bioinks to perform 3D printing of cell-laden structures. To realize the printability, the bioink materials should undergo rapid gelation from fluid state to gel state *in situ* during printing. Normally, two cross-linking strategies are used to realize quick sol-to-gel transition: 1) "A + B" systems with strong binding energy and rapid kinetics of cross-linking (such as alginate+Ca^{2+} ink)[73]; 2) temperature-triggered sol-to-gel transition (gelatin ink)[75]. In those two time-dependent injectable hydrogel systems, it is essential and very challenging to have a strict control over the printing parameters with gelation rate.

To solve the above problems, I applied dynamic coordination strategy in **paper I** to develop HA-BP•Ca^{2+} hydrogel as a bioink that can be easily manufactured into various hydrogel constructs with robotic dispensing printing technique. Due to the shear-thinning properties of HA-BP•Ca^{2+} hydrogel, it can be extruded from a printer nozzle smoothly. To prove the printability of HA-BP•Ca^{2+} hydrogel, it was deposited on a glass surface to build 2-4 layers of two letters structures ("O" and "T") with a home-made syringe extruder (Figure 2.9a). However, it was impossible to print real multi-layered 3D structures under air atmosphere due to too poor mechanical properties of the hydrogel. Therefore, we used physical Am-HA-BP•Ca^{2+} hydrogel as printed material and omnidirectionally print it into a supporting HA-BP•Ca^{2+} gel bath (i.e., embedding gel-into-gel approach). 3D tube-like structure with 100 layers was printed, followed by exposure to UV light to covalently fix the resulting construct. Based on the pH-sensitivity of coordination BP•Ca^{2+} bonds, a

slightly acidic PBS buffer was used to isolate the tube-like structure from HA-BP•Ca^{2+} supporting bath (Figure 2.9b).

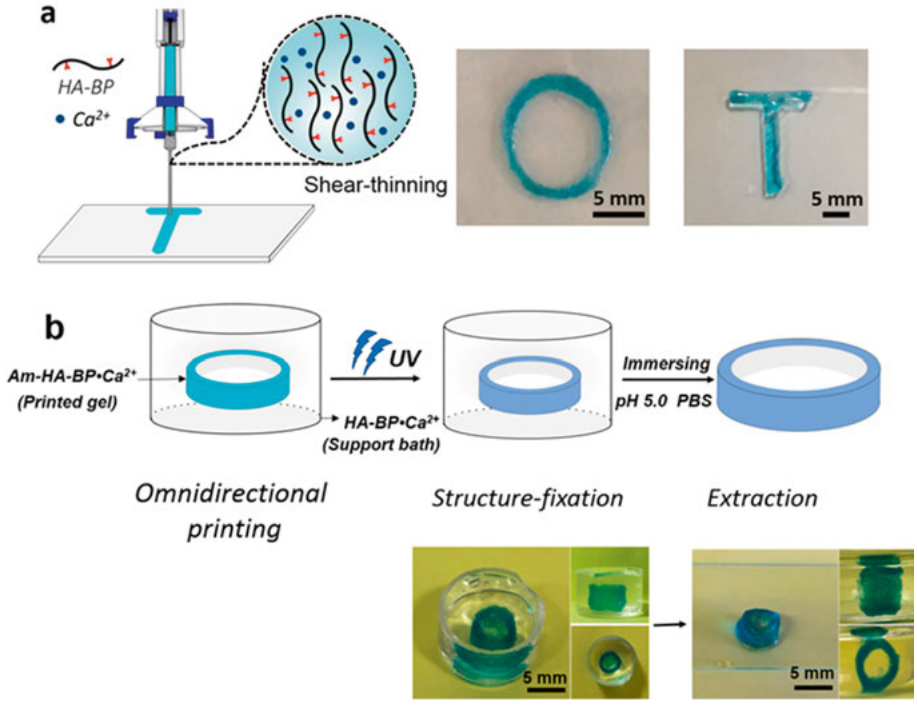

Figure 2.9 (a) HA-BP•Ca^{2+} hydrogel ink was patterned on a glass surface using a home-made extruder. The hydrogel was stained with alcian blue for contrast visualization. (b) 100-layer of tube like structure (Am-HA-BP•Ca^{2+} hydrogel, blue) was directly printed inside support medium of HA-BP•Ca^{2+} hydrogel. The printed structure was fixed by UV light, and then extracted from the supporting bath by incubation in slightly acidic PBS.

To use Am-HA-BP•Ca^{2+} hydrogel as bioink in a real bioprinting applications, it is important to evaluate the viability of living cells after encapsulating them in the 3D hydrogel and the following processing by photochemical *in situ* cross-linking. Therefore, osteoblast-like (MG63) cells were encapsulated in Am-HA-BP based three-type hydrogels: 1) only coordination cross-linked (i.e., +Ca^{2+}/no UV) gel; 2) only UV light induced chemically cross-linked (i.e., no Ca^{2+}/+UV) gel; 3) dually cross-linked (i.e., +Ca^{2+}/+UV) gel. The cell viabilities were tested using live-dead staining assay. MG63 cells could survive very well in coordination cross-linking, photo-mediated radical additional reaction as well as the condition of a combination of above two cross-linkages (Figure 2.10a,b,c,e). After 24 hours culture, the cell viabilities in no Ca^{2+}/+UV gel and +Ca^{2+}/+UV gel were not decreased significantly as compared with those after encapsulating immediately (Figure 2.10a,d,f). In all the groups, MG63 cells had above 88% of viabilities. Moreover, more than 80% of human

adipose-derived stem cells (ASC/TERT1) could survive inside 3D double cross-linked Am-HA-BP•Ca^{2+} hydrogel over 6-day culture (Figure 2.10g-i). The high cell viability in 3D hydrogel culture is the fundamental prerequisite to further exploit this material for 3D bioprinting.

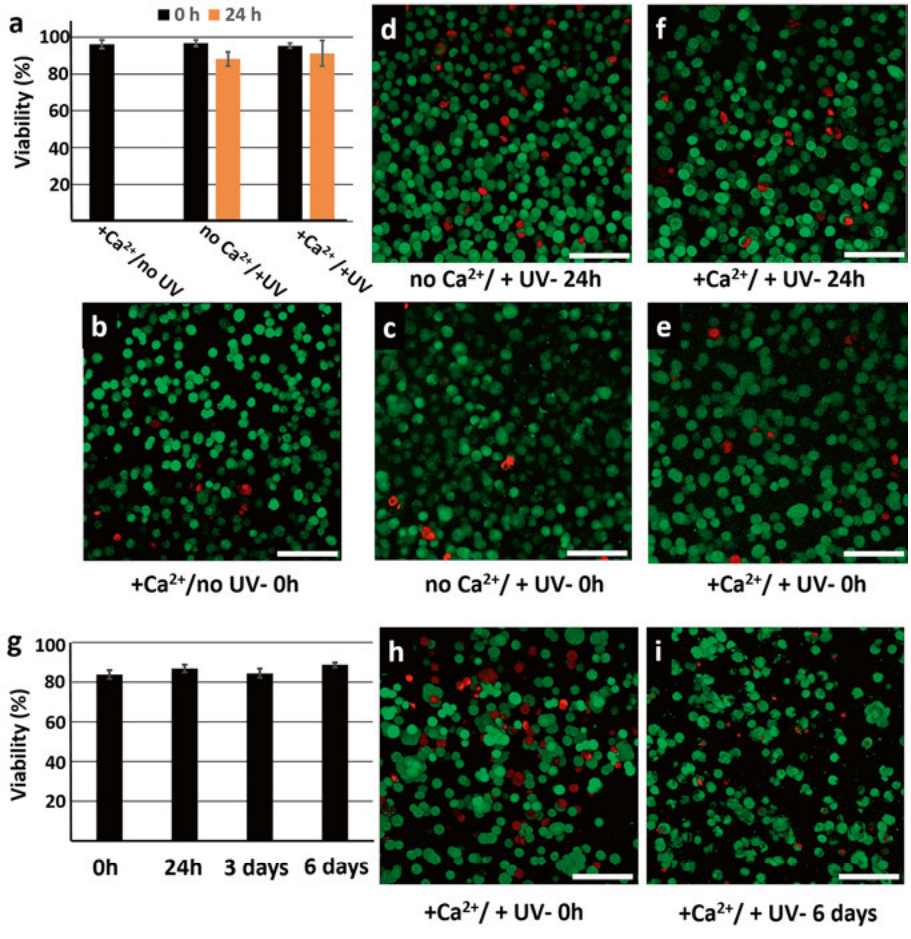

Figure 2.10 (a) The quantified MG63 cells viabilities after 3D culturing them in only coordination cross-linked hydrogel (+Ca^{2+}/no UV), only chemically (no Ca^{2+}/+UV), and dually cross-linked (+Ca^{2+}/+UV) Am-HA-BP hydrogels followed by the 24 h incubation. The images of live-dead staining for MG63 cells in (b) only coordination cross-linked gel (time = 0 h), (c) only chemically cross-linked gel (time = 0 h), (e) dually cross-linked gel (time=0 h), (d) only chemically cross-linked gel (time = 24 h), and (f) dually cross-linked gel (time = 24 h). (g) Cells viabilities for ASC/hTERT cells after 3D culturing in dually cross-linked Am-HA-BP•Ca^{2+} hydrogel over six days. Live-dead staining images of the ASC/hTERT cells after (h) 0 h and (i) 6 days of culturing. Scale bar 100 μm.

2.7 Wound-healing hydrogel

Polymer-based biomaterials have been widely applied as skin regenerative scaffolds to accelerate the healing process for full-thickness wound damages. Hydrogels are able to protect the wound areas from drying, swallow the exudates from wound beds, as well as be readily removed or biodegraded without destroying the structure of the newly healed skin.[76-78] One of the most common GAG in skin matrix, HA, has been proved to participate in many steps of wound healing, for example, inflammation, granulation, and even epithelium regeneration.[79, 80] HA macromolecules afford an environment to arrange fibroblasts and endothelial cells migration as well as proliferation in the preliminary stage of healing.[81] It is also found that HA improves angiogenesis in the process of wound healing.[82, 83] Moreover, many researches demonstrated that HA is particularly involved in scarless healing for fetal damaged skin.[84] Basing on that above knowledge, HA-based hydrogel is an attractive biomaterial for treatment of skin defects. A chemically cross-linked HA based on hydrazone cross-linkage was fabricated by the Prestwich group, which showed the ability to improve reepithelialization in animal model.[85] Moreover, another HA hydrogel cross-linked by Michael addition of acrylate-functionalized HA with a peptide containing two cysteine residues with the porous structure and encapsulating biological factor plasmid was developed to treat skin defect in diabetic mouse.[86] However, these two HA hydrogels based on covalent cross-linkages do not demonstrate reversible properties such as self-healing and moldability.

In **paper II**, HA-BP•Ag^+ hydrogel was applied on the surface of the rat full-thickness skin defect over 10 days and the healing process was monitored by digital camera. We calculated the wound remaining rates at various time points (i.e., 3-,6-, 10-day) normalizing with the initial wound size created by surgery (Figure 2.11a). Control group without receiving any materials treatment revealed lower wound remaining rate in comparison with HA-BP•Ag^+ group on 3-day (Figure 2.11a), which might be caused by the shrinkage of the opened wound beds of control group because of drying effect rather than the real regeneration induced closure. The remaining wounds rates in hydrogel-treated group declined from 77.8 ± 3.7% to 48.2 ± 3.7% (n=4) in the course from 3-day to 6-day, while those in control group were only decreased from 68.6 ± 9.4% to 58.5 ± 4.0% (n=4). On 10-day, remaining wound rates in HA-BP•Ag^+ group were13.0 ± 1.2% that were significantly (*$P < 0.05$) lower than 22.6 ± 2.9% of remaining rates in control group (Figure 2.11a). Furtherly, we used hematoxylin and eosin (H&E) reagents to stain the sample collected at 10-day after surgery and observed the histological difference between hydrogel-treated group and control group. The results displayed that the thickness of the newly regenerated epidermal layer (i.e., 144.4 ± 32.5 μm) in HA-BP•Ag^+ group was significantly (**$P < 0.01$) bigger than 63.8 ± 32.4 μm

thickness in control group (Figure 2.11b). According to above data, we conclude, therefore, that HA-BP•Ag^+ clearly showed skin regeneration capability in a full-thickness wound model.

One of the main issues for wound healing care is bacterial-induced infection. Therefore, skin regenerating biomaterials usually include antimicrobial agents to provide the anti-bacterial properties. Based on results of disk diffusion experiments, our HA-BP•Ag^+ hydrogel showed obvious inhibition activities against both Gram-positive (*Staphylococcus aureus*) and Gram-negative (*Escherichia coli*) bacteria, which were contributed by silver ions with well-known antibacterial properties (Figure 2.11c).

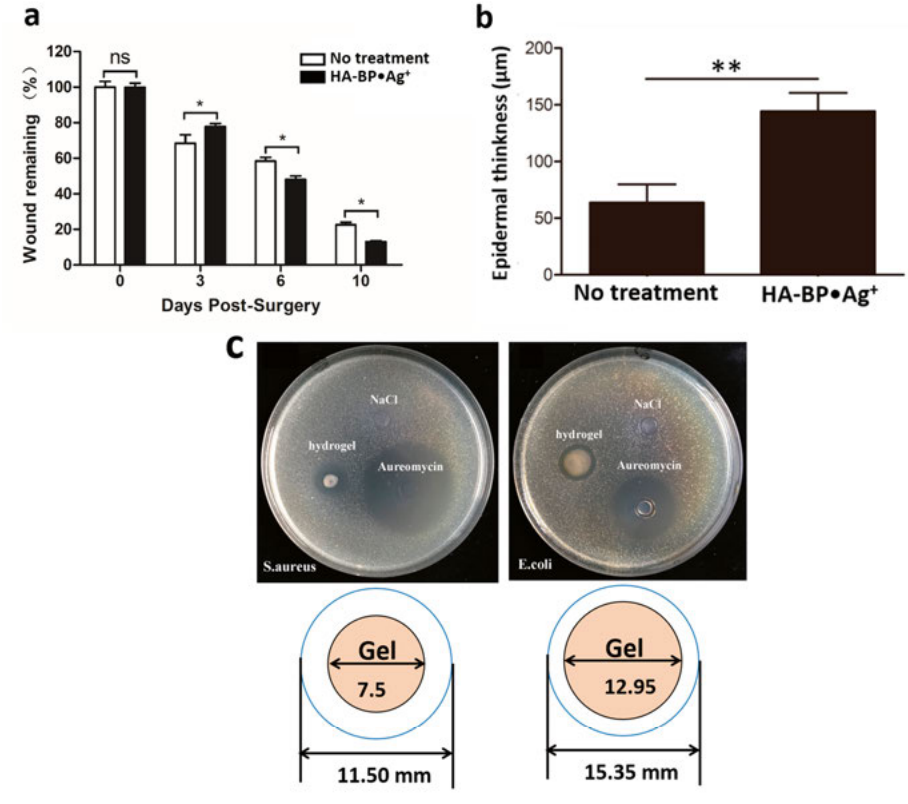

Figure 2.11 (a) Percentages of remaining wound areas in both HA-BP•Ag^+ hydrogel group and no treatment group at 3-, 6- and10-day relative to the initial wound size at 0-day. Asterisks (*) represented the statistically significant difference between the group received hydrogel treatment and the group without hydrogel treatment ($n = 4$, $*P < 0.05$). (b) Quantitative measurement of newly healed epidermal layers basing on H&E staining at day 10 post-surgery ($n = 4$, $**P < 0.01$). (c) Inhibition zones induced by HA-BP•Ag^+ hydrogel was clearly observed by the disk diffusion test. Aureomycin and NaCl were selected as positive and negative control, respectively.

2.8 Bone-regenerative scaffold

A tissue engineering approach basing on osteoinductive biomaterials is one of the most promising strategies to repair a damaged bone, revolutionizing the traditional bone regeneration methods. Currently, three main biomaterials categories are commonly used for bone repair: 1) ceramic-based materials; 2) polymer-based materials; 3) the materials based on the combination of ceramic and polymer.[87, 88] Due to the great biocompatibility, tunable biodegradation and easy functionalization, various polymers have been widely applied in preparation of bone regenerating biomaterials. Particularly, polymer-based hydrogel materials with injectable properties may offer the minimally invasive of bone-inducing factors, thus attracting much attention of clinicians.[89, 90]

In **paper III**, the HA-BP•CaP@mSF hydrogel was fabricated by simple mixing under physiological environment, and exhibited a unique hierarchical bone-mimicking composed of a polysaccharide, a protein, and a CaP-based mineral. To evaluate its osteogenesis abilities, we applied the Am-HA-BP•CaP@mSF hydrogels doubly cross-linked with both coordination and covalent bonds on rat cranial critical defect (diameter: 8 mm) model and the newly regenerated bone volume was estimated using micro-CT at 4- and 8-week post-implantation. After 4 weeks of implantation, the newly formed bone was only observed in the hydrogel-tissue interface area in the hydrogel-treated group (Figure 2.12a), while there was not any appreciable bone-like tissue at the group without treatment (Figure 2.12b). With the time increasing from 4 weeks to 8 weeks, the bone formation increased further (Figure 2.12c,d). Although the hydrogel unfilled group showed new bone formation over 8 weeks post-surgery (Figure 2.12d), the amount of newly regenerated bone was significantly lower than that in the hydrogel implanted group (Figure 2.12i). Based on the bone quantitative measurement, the newly bone volumes were 4.17 ± 0.85 and 0.93 ± 0.54 mm^3 after 4 weeks for the hydrogel treated and unfilled groups, respectively. After 8 weeks, these two values were significantly increased to 7.65 ± 2.5 and 3.0 ± 0.42 mm^3 for the hydrogel treated and untreated groups, respectively (Figure 2.12i). The images of sagittal cross-sections also confirmed the healing process after hydrogel implantation in the course from 4 weeks to 8 weeks (Figure 2.12e–h). Osteoblast-like cells, as well as vessel-like tissues, were observed after hematoxylin and eosin (H&E) staining in the hydrogel implantation group after 8 weeks, which further confirmed the bone formation.

Therefore, the results from micro-CT analysis and histological observation demonstrated that the doubly cross-linked Am-HA-BP•CaP@mSF hydrogel promoted *in vivo* osteogenesis even without the addition of growth factors and cells. The inorganic CaP composition on the surface of silk fibers could contribute the bone formation, which has the similar amorphous structure to the bone in the body. Although the mechanical properties of the presented hydrogel are much lower than that of real bone structure, it's able to provide

an injectable scaffold to fill orthopaedic cavities for non-load bearing bone healing applications.

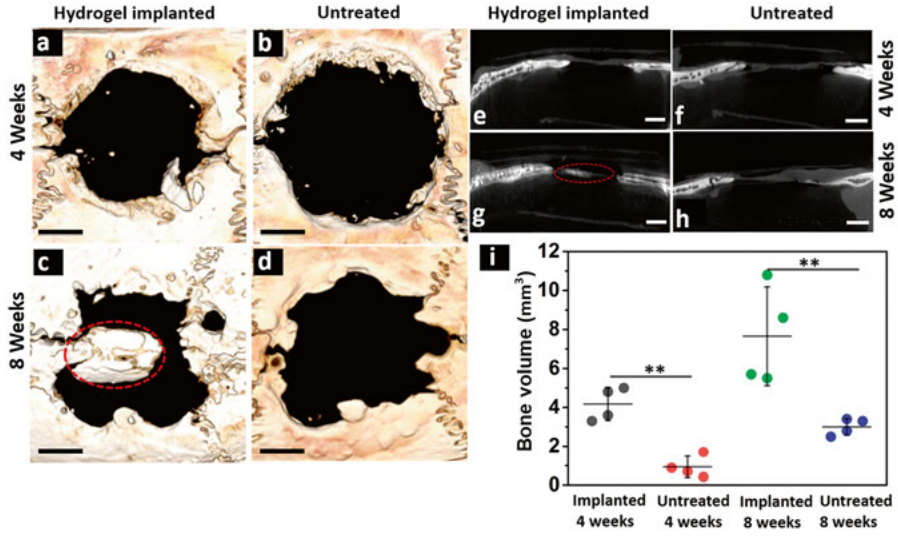

Figure 2.12 Bone formation induced by doubly cross-linked Am-HA-BP•CaP@mSF hydrogel in a rat cranial defect model basing on Micro-CT analysis: (a-d) 3D reconstruction images and (e-h) sagittal cross-section images. (i) Quantification of bone volume for the newly regenerated bone. All data were demonstrated by means ± SD (n= 4, **p < 0.01)

2.9 Drug delivery system

Drug delivery systems are promising tools to realize drug's controllable release, being able to reduce the drug toxicities to the healthy cells or tissues. Moreover, encapsulating therapeutic molecules inside a high water content system, such as a hydrogel, can protect them from inactivation. Hydrogel-based drug delivery system exhibits not only tunable releasing speed controlled by cross-linking density of the network and interaction between drugs and hydrogel matrix but also potential injectable properties that can provide minimally invasive delivery.[91, 92]

In **paper IV**, we applied our composite HA-BP•$MgSiO_3$ hydrogel as drug delivery system using $MgSiO_3$ NPs with high drug loading efficiency provided by their mesoporous structure. To prepare the drug loaded injectable hydrogel, doxorubicin (Dox) was firstly loaded inside $MgSiO_3$ NPs and the hydrogel was then formed by mixing Dox-loaded $MgSiO_3$ (MgSiO3@Dox) NPs dispersion with HA-BP solution. In our hydrogel drug delivery system, $MgSiO_3$ NPs act as both drug carriers and cross-linkers of hydrogel network. Additionally, the particles release experiments were performed in acidic environment (pH=5.0) and in natural medium (pH=7.4) over different time points

(i.e., 2, 4, 8, and 24 hours). The mass of $MgSiO_3$ NPs released from hydrogel was measured at each time point (Figure 2.13a). The $MgSiO_3$ NPs were gradually released in pH=5.0 medium due to the protonation of BP groups and the subsequent breaking of coordinate cross-linkage (Figure 2.13a,b). On the other hand, the HA-BP•$MgSiO_3$ hydrogel exhibited great stability in neutral environment (Figure 2.13a,b). Based on the slight acidic pH value in the tumor's microenvironment, the presented hydrogel with pH-sensitive particle release feature is quite suitable to serve as the anti-cancer drug delivery system.

To investigate the anti-cancer properties of HA-BP•$MgSiO_3$@Dox hydrogel, human breast cancer cells (MCF-7) were treated with the released medium obtained from HA-BP•$MgSiO_3$@Dox hydrogel at pH 5.0. To exclude the influence of drug-free hydrogel on killing cancer cells, a negative control group was included using the released medium from HA-BP•$MgSiO_3$ hydrogel. The released medium obtained from HA-BP•$MgSiO_3$@Dox hydrogel at all collected time points showed significantly inhibition effect on MCF-7 cells compared with the released medium from Dox-free hydrogel (Figure 2.13c). Moreover, more than 80% cell viabilities in the group of hydrogel without loaded Dox demonstrated the minor cytotoxicity of $MgSiO_3$ NPs (Figure 2.13c). Additionally, internalization of $MgSiO_3$@Dox NPs by MCF-7 cells was proven after 3-hour incubation based on the fluorescence microscopy observation.

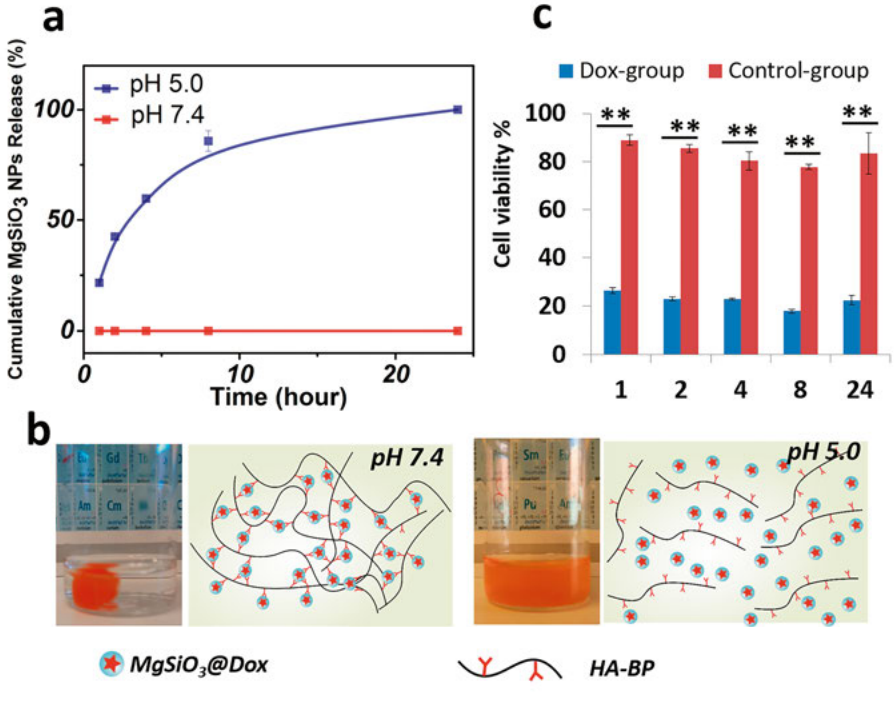

Figure 2.13 (a) Curve of $MgSiO_3$ NPs release from the HA-BP•$MgSiO_3$ composite hydrogel in acidic and neutral media (pH = 5.0 and pH = 7.4). (b) Images of HA-

BP•MgSiO3@Dox hydrogel after incubation in PBS at pH = 5.0 and pH = 7.4. (c) Viability of MCF-7 cells after incubation over 24 hours with released medium obtained from various collecting time points from drug-loaded (blue bars) and drug-free (red bars) hydrogels. The statistical difference was given as **$p < 0.01$.

3 Concluding remarks and future perspectives

Injectable hydrogels have been widely investigated for various biomedical applications due to the advantage for minimally invasive delivery. In this thesis, metal-ligand coordination assembling approach was used to fabricate a family of injectable hydrogels with unlimited time window for injection. We applied the resulting injectable hydrogels in four different biomedical areas including 3D printing, skin regeneration, bone healing and drug delivery. The reason for the hydrogels with dynamic properties (i.e., shear-thinning and self-healing properties) is the reversibility of coordination cross-linkages.

To realize the coordination cross-linkages, bisphosphonate group as a ligand was conjugated onto the backbones of hyaluronic acid to obtain the HA-BP derivatives (**Figure 2.1**). In this thesis, the EDC coupling reactions were used to make three different HA derivatives firstly, namely, HA-SH, HA-SSPy and HA-Mal. The HA-BP derivatives with slightly different branched structures were then obtained from HA-SH, HA-SSPy, and HA-Mal using thiol-ene addition reaction, thiol-disulfide ex-change reaction and "click"-type Michael addition, respectively. Moreover, the dually functionalized HA derivatives with both BP group and acrylamide group (i.e., Am-HA-BP) were synthesized by two different chemical reaction pathways (**Figure 2.2**).

In **paper I**, the injectable hydrogel was formed by simple mixing of HA-BP or Am-HA-BP polymer liquid and $CaCl_2$ solution. Based on the rheology results, HA-BP•Ca^{2+} and Am-HA-BP•Ca^{2+} hydrogel showed the shear-thinning and self-healing properties. We manufactured multi-layered 3D tube-like construct by embedding the printed material (Am-HA-BP•Ca^{2+} gel) into supporting bath (HA-BP•Ca^{2+} gel) using home-modified 3D printer. To fix the structure of the printed 3D structure, UV-light was applied after printing to covalently cross-link the hydrogel networks. The cell experiments results exhibited that bone osteosarcoma cells and stem cells can survive after 3D encapsulation into Am-HA-BP•Ca^{2+} gel and the consequent photo cross-linking.

In **Paper II**, Ag^+ ions were introduced into HA-BP solution to develop the HA-BP•Ag^+ hydrogel. Based on the dynamic features of BP•Ag^+ coordination, the resulting HA-BP•Ag^+ hydrogel exhibited self-healing properties and moldability. Moreover, the hydrogel could kill both *S.aureus* and *E.coli* bacteria, exhibiting a broad-spectrum antibacterial property. In rat skin full-thickness defect model, HA-BP•Ag^+ hydrogel significantly accelerated the wound healing process and enhanced the thickness of the newly regenerated epidermal layer.

In **paper III**, the bone mimicking injectable hydrogel was fabricated based on the Am-HA-BP polymer and calcium phosphate coated silk microfibers (i.e., CaP@mSF). The Am-HA-BP•CaP@mSF hydrogel can be delivered through a thin needle and its mechanical properties and structure integrities were improved by a doubly cross-linked network containing both coordination and covalent cross-linkages. The presented double cross-linked Am-HA-BP•CaP@mSF hydrogel induced the bone regeneration even without any cells and growth factors addition in the rat cranial critical defect model.

In **paper IV**, $MgSiO_3$ NPs with mesoporous structure was prepared to load the anti-cancer drug, doxorubicin (Dox). The drug-loaded hydrogel was prepared by mixing of HA-BP solution and $MgSiO_3$@Dox dispersion. Rheology results demonstrated that two essential factors were required for the hydrogel formation: BP groups on the HA polymer and Mg^{2+} ions on NPs. The MgSiO3@Dox NPs were released from the hydrogel in acidic buffer and the particles were internalized by cancer cells to induce the toxic response.

In summary, I used dynamic coordination approaches to develop shear-thinning and self-healing hydrogels based on the cross-linking between the BP groups on the backbones of HA molecules and various metal cations or metal slats particles. The presented family of coordination hydrogels exhibited time-independent injection behaviors, and can serve as 3D printing bioinks, regenerative medicine materials and drug delivery systems.

3.1 Ongoing studies

Although four different biomedical applications have been demonstrated in this thesis using HA-BP based coordination hydrogels, it is still too far to apply them in real clinical applications. For example, it is too difficult to delivery UV-light into the human body by a minimally invasive approach. Therefore, developing of chemical methods to form the secondary covalently cross-linked network *in vivo* without the use of UV light is one of the several interesting studies for the future. It was found that the cells can survive in 3D Am-HA-BP•Ca^{2+} hydrogel, however, the cellular morphology was round, meaning that the cells were not attached to the hydrogel network. Therefore, it is needed to improve the hydrogel of adhesion to cells by incorporation of gelatin or arginylglycylaspartic acid (RGD) peptides. Additionally, to expand the applications in biomedical area, we are planning to exploit HA-BP based hydrogels to print vascularized tumor models and prepare tissue- or tumor-on-chips.

4 Acknowledgement

When I started to write this part, so many names came to my mind. The four-year Ph.D life in Uppsala, a very beautiful city, contains so many exciting scientific experiences as well as wonderful life memories. I got many supports and helps from colleagues, friends and my family, and I would like to express my sincere gratitude to them.

First of all, I would like to express my heartfelt gratitude to my main supervisor, Prof. Jöns Hilborn, for providing me the opportunity for working in polymer chemistry group. Thanks a lot for many critical and very useful comments and suggestions from you for my experiments, manuscripts, and thesis. Your guidance for presentation skills and my career planning are really valuable. Moreover, I really enjoyed the freedom you gave me to perform any projects I like.

Then, I would like to express my sincere gratitude to another important supervisor, Dmitri Ossipov, for guidance and help during my whole Ph.D studies. Your talents to researches, your hard-working attitude, and your patience to students impress me a lot. Whenever I got questions for my researches, you always gave me helps very quickly. To be honest, I did not have many experiences for conduction organic reactions before I came polymer group. I really appreciated that you taught me carefully and patiently how to perform chemical reaction. I have learnt a lot from you including experiments skills, chemical knowledge, manuscript writing and so on. I really enjoyed the discussion with you in our fika time almost each afternoon. Many fantastic maybe crazy ideas actually came from that time. Thank you very much!

I would like to thank Tim Bowden for your critical comments and suggestions during my presentations in the group meeting. I also want to thank Oommen Varghese to give me many suggestions for my research and career and going through my thesis. Thanks to Janne for fixing the broken instruments in the lab and for making silicon model for my silk scaffold. Special thanks to Shujiang for lots of conversations for both science and life, as well as for revising my thesis. Yu, thank you for teaching me how to set up reactions and for many good suggestions to live in Sweden when I just came to this country. I really liked the hotpot and noodle you prepared. Thank Youka for helping me when I looked for PhD position and also for teaching me the preparation of liposome. Ayan, thank you for your help in Grammarly software use and for your suggestions for my thesis. I also would like to express my gratitude for other group membranes in polymer chemistry: O.P., Sujit, Sandeep,

Ganesh, Daniel, Andreas, Maruthi, Hongji, Justina, Xufeng, Yan, Ming, Hannah, Rekha, etc.

I would like to thank all my collaborators in my Ph.D studies. Thank Prof. Jianwu Dai and Dr. Yannan Zhao to perform animal wound healing experiments. Thank Prof. Xisheng Weng and Dr. Wei Zhu for conduction of experiments of bone regeneration *in vivo*. Thank Prof. Sabine Fuchs, Fanlu Wang, Dr. Aleksandr Ovsianikov, Katja Hölzl for the cell experiments. Thank Hauke Carstensen for modification the 3D printer extruder. Thank Prof. Heinz Redl and Dr. Andreas Teuschl for accepting me as a short visiting student to work in your lab in Vienna.

I appreciate the China Scholarship Council to provide me the four-year living cost in Sweden. I also appreciate the travel grants from Anna Maria Lundin, Liljewalch and ÅForsk foundation.

I would like to express my sincere gratitude to my dear Chinese friends in Uppsala: Yuanyuan Han, Dan Wu, Dou Du, Xiao Yang, Le Fu, Tianbo Duan, Bo Cao, Cui Li, Ling Xie, Bo Tian, Zhaohui Wang, Wei Xia, Kai Hua, Chenyu Wen, Shengyang Zhou, Chao Xu, Tianfei Liu, Shihuai Wang, Bo Xu, Weijia Yang, Wen Huang, Hailiang Fang, Hao Cao, Mingzhi Jiao, Hu Li, Feiyan Liang, Fengzhen Sun, Peng Zhang, Teng Zhang, Junxin Wang, Jiaojiao Yang & Jun Luo, Zhen Qiu & Zhicheng Wang, Ruijun Pan & Qiuhong Wang, Son Chen & Shu Li, Yi Ren & Xiaowen Li, Meiyuan Guo & Yuhan Ma, Qifan Xie & Huiying Qu, Lei Tian & Rui Sun. I wish you guys all the best in your future.

Finally, I would like to express my sincere gratitude to my whole family. Thank my parents to give always me the best you had for supporting on my life and study. My parents in law, thank you for the solid support on my Ph.D studies. I would like to express my heartfelt appreciation to my wife, Jingyi, and our soon coming baby. Thank you for the love you gave me. Love all of you forever!

特别感谢我的父母、岳父母以及其他关心我的家人们给予我学业和生活的巨大支持。感谢我挚爱的妻子和将要出生的宝宝，是你们给了我前进的巨大动力，我永远爱你们！

5 Svensk sammanfattning

Denna avhandlingen presenterar nya strategier för injicerbara hydrogeler och exempel på användning inom biomedicinska applikationer, såsom 3D-tryck, regenerativ medicin och läkemedelsleverans. Hydrogelerna som är tvärbundna med dynamiska metalligand koordinationsbindningar uppvisar ett skjuvförtunnande och självläkande beteende, vilket resulterar i ett oberoende av tidpunkten för injektion. Till skillnad från permanent tvärbundna nätverk baserat på injektion av vätskeformiga prepolymera lösningar som när de blandas bildar ett kovalent nätverk, kan våra hydrogeler injiceras redan från sitt tvärbundna geltillstånd.

Hyaluronsyra (HA) har valts som polymer baserat på dess biokompatibilitet och nedbrytbarhet. HA har modifierats genom att funktionalisera polymeren med bisfosfonat (BP) som ligand för kelatering av metalljoner eller metallsalt för att kunna bilda koordinationstvärbindningar. I den första delen av avhandlingen har jag utvecklat nya kemiska metoder för att syntetisera BP-funktionell HA och HA med två olika funktionella grupper, BP och akrylamid (Am-HA-BP). Strukturen hos HA-BP verifierades med NMR där specifikt metylgruppen på det grenade kolet i BP vid 2.18ppm i ^{1}H-NMR spektrat använts samt fosfortoppen vid 18.27 ppm i ^{31}P-NMR. I avhandlingens följande del beskrivs hydrogeler som bildats genom HA-BP eller Am-HA-BP genom att tillsätta kalciumsalt (Publikation I), silversalt (Publikation II), mikrofibrer av silke täckta med kalciumfosfat (CaP@mSF) (Publikation III), och magnesiumsilikatpartiklar (Publikation IV). Hydrogelerna karaktäriserades med reologi som visade dynamiska egenskaper vid försök med varierande mekanisk belastning och variation av tid. Detta är ett resultat av reversibiliteten hos tvärbindningarna och bindning mellan BP och metaljonen eller metallsalt på ytan av partiklarna. I den sista delen av avhandlingen behandlas användning av gelerna för biomedicinska applikationer. Am-HA-BP•Ca^{2+} hydrogelen extruderades med en modifierad 3D printer och fixerades sedan med UV för att bilda en multilagerbaserad tub (Publikation I). I en fulltjockleks huddefekter på råtta visades att HA-BP•Ag^{+} påskyndar sårläkningsprocessen och ger en ökad tjocklek på den regenererade överhuden (Publikation II). I kraniell defekt på råtta användes Am-HA-BP•CaP@mSF utan ytterligare biologiska faktorer för att inducera benbildning (Publikation III). En HA-BP gel bildades med magnesiumsilikatpartiklar som laddats med cancermedicin. Partiklarna visade upptag i cancerceller och signifikant ökad toxicitet för laddade partiklar (Publikation IV).

Sammanfattningsvis presenterar avhandlingen kemiska strategier för att använda metallers interaktioner med ligander för att bilda hydrogeler med dynamiska kemiska bindningar och därmed erhålla tidsoberoende injektionsegenskaper. Den här typen av hydrogeler öppnar för nya biomedicinska möjligheter.

6 References

1. Ghorbanali, S.; Hossein, H. *Advanced Healthcare Materials* **2017**, 6, 1700801.
2. Hoare, T. R.; Kohane, D. S. *Polymer* **2008**, 49, 1993-2007.
3. Hölzl, K.; Lin, S.; Tytgat, L.; Van Vlierberghe, S.; Gu, L.; Ovsianikov, A. *Biofabrication* **2016**, 8, 032002.
4. Zuan-Tao, L.; Jianhua, G.; Chien-Hung, L.; Randall, L. T.; Lixin, X.; Shuo, C.; Piao-Yang, C.; Shan, J.; Yulin, Y.; Xia, H.; Hongting, W.; Dezhi, W.; Xifan, W.; Gang-Biao, J.; Mikala, H.; Tianfu, W. *Advanced Materials* **2017**, 29, 1702090.
5. Kristoffer, B.; Thomas, E.; Jöns, H.; Dmitri, O.; Sonya, P.; Tim, B. *Journal of Biomedical Materials Research Part A* **2009**, 91A, 1111-1118.
6. Buwalda, S. J.; Vermonden, T.; Hennink, W. E. *Biomacromolecules* **2017**, 18, 316-330.
7. Silva, A. K. A.; Richard, C.; Bessodes, M.; Scherman, D.; Merten, O.-W. *Biomacromolecules* **2008**, 10, 9-18.
8. Wang, L. L.; Sloand, J. N.; Gaffey, A. C.; Venkataraman, C. M.; Wang, Z.; Trubelja, A.; Hammer, D. A.; Atluri, P.; Burdick, J. A. *Biomacromolecules* **2016**, 18, 77-86.
9. Dimatteo, R.; Darling N.J.; Tatiana S. *Advanced Drug Delivery Reviews* **2018**, 127, 167-184.
10. Billiet, T.; Vandenhaute, M.; Schelfhout, J.; Van Vlierberghe, S.; Dubruel, P. *Biomaterials* **2012**, 33, 6020-6041.
11. Yang, J.-A.; Yeom, J.; Hwang, B. W.; Hoffman, A. S.; Hahn, S. K. *Progress in Polymer Science* **2014**, 39, 1973-1986.
12. Nguyen, Q. V.; Park, J. H.; Lee, D. S. *European Polymer Journal* **2015**, 72, 602-619.
13. Zhang, Y.; Rossi, F.; Papa, S.; Violatto, M. B.; Bigini, P.; Sorbona, M.; Redaelli, F.; Veglianese, P.; Hilborn, J.; Ossipov, D. A. *Acta biomaterialia* **2016**, 30, 188-198.
14. Kim, M.; Lee, J. Y.; Jones, C. N.; Revzin, A.; Tae, G. *Biomaterials* **2010**, 31, 3596-3603.
15. Takahashi, A.; Suzuki, Y.; Suhara, T.; Omichi, K.; Shimizu, A.; Hasegawa, K.; Kokudo, N.; Ohta, S.; Ito, T. *Biomacromolecules* **2013**, 14, 3581-3588.
16. Ossipov, D. A.; Brännvall, K.; Forsberg-Nilsson, K.; Hilborn, J. *Journal of applied polymer science* **2007**, 106, 60-70.
17. Shi, D.; Xu, X.; Ye, Y.; Song, K.; Cheng, Y.; Di, J.; Hu, Q.; Li, J.; Ju, H.; Jiang, Q. *ACS nano* **2016**, 10, 1292-1299.
18. Burdick, J. A.; Anseth, K. S. *Biomaterials* **2002**, 23, 4315-4323.
19. Lin, H.; Cheng, A. W.-M.; Alexander, P. G.; Beck, A. M.; Tuan, R. S. *Tissue Engineering Part A* **2014**, 20, 2402-2411.
20. Guvendiren, M.; Lu, H. D.; Burdick, J. A. *Soft matter* **2012**, 8, 260-272.
21. Appel, E. A.; del Barrio, J.; Loh, X. J.; Scherman, O. A. *Chemical Society Reviews* **2012**, 41, 6195-6214.
22. Wang, H.; Heilshorn, S. C. *Advanced Materials* **2015**, 27, 3717-3736.

23. Krogsgaard, M.; Nue, V.; Birkedal, H. *Chemistry-A European Journal* **2016**, 22, 844-857.
24. Zhang, J.; Su, C.-Y. *Coordination Chemistry Reviews* **2013**, 257, 1373-1408.
25. Harrington, M. J.; Masic, A.; Holten-Andersen, N.; Waite, J. H.; Fratzl, P. *Science* **2010**, 328, 216-220.
26. Holten-Andersen, N.; Harrington, M. J.; Birkedal, H.; Lee, B. P.; Messersmith, P. B.; Lee, K. Y. C.; Waite, J. H. *Proceedings of the National Academy of Sciences* **2011**, 108, 2651-2655.
27. Li, Q.; Barrett, D. G.; Messersmith, P. B.; Holten-Andersen, N. *ACS nano* **2016**, 10, 1317-1324.
28. Grindy, S. C.; Holten-Andersen, N. *Soft matter* **2017**, 13, 4057-4065.
29. Wei, Z.; He, J.; Liang, T.; Oh, H.; Athas, J.; Tong, Z.; Wang, C.; Nie, Z. *Polymer Chemistry* **2013**, 4, 4601-4605.
30. Gerth, M.; Bohdan, M.; Fokkink, R.; Voets, I.; van der Gucht, J.; Sprakel, J. *Macromolecular rapid communications* **2014**, 35, 2065-2070.
31. Highley, C. B.; Rodell, C. B.; Burdick, J. A. *Advanced Materials* **2015**, 27, 5075-5079.
32. Yamaguchi, H.; Kobayashi, Y.; Kobayashi, R.; Takashima, Y.; Hashidzume, A.; Harada, A. *Nature communications* **2012**, 3, 603.
33. Nakahata, M.; Takashima, Y.; Yamaguchi, H.; Harada, A. *Nature communications* **2011,** 2, 511.
34. Harada, A.; Kobayashi, R.; Takashima, Y.; Hashidzume, A.; Yamaguchi, H. *Nature chemistry* **2011**, 3, 34-37.
35. Appel, E. A.; Loh, X. J.; Jones, S. T.; Dreiss, C. A.; Scherman, O. A. *Biomaterials* **2012**, 33, 4646-4652.
36. Ma, X.; Zhao, Y. *Chemical reviews* **2014**, 115, 7794-7839.
37. Diba, M.; Spaans, S.; Ning, K.; Ippel, B. D.; Yang, F.; Loomans, B.; Dankers, P. Y.; Leeuwenburgh, S. C. *Advanced Materials Interfaces* **2018**, 1800118.
38. Steed, J. W.; Atwood, J. L., *Supramolecular chemistry*. John Wiley & Sons: 2013.
39. Bastings, M.; Koudstaal, S.; Kieltyka, R. E.; Nakano, Y.; Pape, A.; Feyen, D. A.; Van Slochteren, F. J.; Doevendans, P. A.; Sluijter, J. P.; Meijer, E. *Advanced healthcare materials* **2014**, 3, 70-78.
40. Kieltyka, R. E.; Pape, A.; Albertazzi, L.; Nakano, Y.; Bastings, M. M.; Voets, I. K.; Dankers, P. Y.; Meijer, E. *Journal of the American Chemical Society* **2013**, 135, 11159-11164.
41. Kretsinger, J. K.; Haines, L. A.; Ozbas, B.; Pochan, D. J.; Schneider, J. P. *Biomaterials* **2005**, 26, 5177-5186.
42. Salick, D. A.; Pochan, D. J.; Schneider, J. P. *Advanced Materials* **2009**, 21, 4120-4123.
43. Haines-Butterick, L.; Rajagopal, K.; Branco, M.; Salick, D.; Rughani, R.; Pilarz, M.; Lamm, M. S.; Pochan, D. J.; Schneider, J. P. *Proceedings of the National Academy of Sciences* **2007**, 104, 7791-7796.
44. Foo, C. T. W. P.; Lee, J. S.; Mulyasasmita, W.; Parisi-Amon, A.; Heilshorn, S. C. *Proceedings of the National Academy of Sciences* **2009**, 106, 22067-22072.
45. Parisi-Amon, A.; Mulyasasmita, W.; Chung, C.; Heilshorn, S. C. *Advanced healthcare materials* **2013**, 2, 428-432.
46. Cai, L.; Dewi, R. E.; Heilshorn, S. C. *Advanced functional materials* **2015**, 25, 1344-1351.
47. Wang, Q.; Wang, L.; Detamore, M. S.; Berkland, C. *Advanced Materials* **2008**, 20, 236-239.
48. Wang, Q.; Wang, J.; Lu, Q.; Detamore, M. S.; Berkland, C. *Biomaterials* **2010**, 31, 4980-4986.

49. Wang, H.; Hansen, M. B.; Löwik, D. W.; van Hest, J.; Li, Y.; Jansen, J. A.; Leeuwenburgh, S. C. *Advanced materials* **2011**, 23, H119–H124
50. Wang, H.; Zou, Q.; Boerman, O. C.; Nijhuis, A. W.; Jansen, J. A.; Li, Y.; Leeuwenburgh, S. C. *Journal of Controlled Release* **2013**, 166, 172-181.
51. Fantner G. E.; Hassenkam T.; Kindt J. H.; Weaver J. C.; Birkedal H.; Pechenik L.; Cutroni J. A.; Cidade G. A. G.; Stucky G. D.; Morse D. E.; Hansma P. K. *Nat. Mater.* **2005**, 4, 612–616.
52. Schofield R.; Lefevre H. *J. Exp. Biol.* **1989**, 144, 577-581.
53. Degtyar, E.; Harrington, M. J.; Politi, Y.; Fratzl, P. *Angewandte Chemie International Edition* **2014**, 53, 12026-12044.
54. Ossipov, D. A. *Expert opinion on drug delivery* **2015**, 12, 1443-1458.
55. Gałęzowska, J. *ChemMedChem* **2018**, 13, 289-302.
56. Zeevaart, J. R.; Jarvis, N. V.; Louw, W. K.; Jackson, G. E.; Cukrowski, I.; Mouton, C. J. *Journal of inorganic biochemistry* **1999**, 73, 265-272.
57. De Rosales, R. T. M.; Finucane, C.; Mather, S.; Blower, P. *Chemical Communications* **2009**, 4847-4849.
58. Laurent T. C. *Upsala J Med Sci*, **2007**, 112, 123-142.
59. Meyer, K.; Palmer, J. W. *Journal of Biological Chemistry* **1934**, 107, 629-634.
60. Liu, L.; Liu, Y.; Li, J.; Du, G.; Chen, J. *Microbial cell factories* **2011**, 10, 99.
61. Balazs, E.; Freeman, M.; Klöti, R.; Meyer-Schwickerath, G.; Regnault, F.; Sweeney, D. *Modern problems in ophthalmology* **1972**, 10, 3.
62. Chen, W. J.; Abatangelo, G. *Wound Repair and Regeneration* **1999**, 7, 79-89.
63. Toole, B. P. Seminars in cell & developmental biology, Elsevier: **2001**, 79-87.
64. Toole, B. P. *Nature Reviews Cancer* **2004**, 4, 528.
65. Kundu, B.; Rajkhowa, R.; Kundu, S. C.; Wang, X. *Advanced drug delivery reviews* **2013**, 65, 457-470.
66. Mottaghitalab, F.; Hosseinkhani, H.; Shokrgozar, M. A.; Mao, C.; Yang, M.; Farokhi, M. *Journal of Controlled Release* **2015**, 215, 112-128.
67. Rockwood, D. N.; Preda, R. C.; Yücel, T.; Wang, X.; Lovett, M. L.; Kaplan, D. L. *Nature protocols* **2011**, 6, 1612.
68. Altman, G. H.; Diaz, F.; Jakuba, C.; Calabro, T.; Horan, R. L.; Chen, J.; Lu, H.; Richmond, J.; Kaplan, D. L. *Biomaterials* **2003**, 24, 401-416.
69. Pins, G. D.; Christiansen, D. L.; Patel, R.; Silver, F. H., Self-assembly of collagen fibers. *Biophysical journal* **1997**, 73, 2164-2172.
70. Engelberg, I.; Kohn, J. *Biomaterials* **1991**, 12, 292-304.
71. Zheng, Z.; Wu, J.; Liu, M.; Wang, H.; Li, C.; Rodriguez, M. J.; Li, G.; Wang, X.; Kaplan, D. L. *Advanced healthcare materials* **2018**, 7, 1701026
72. Pal, R. K.; Farghaly, A. A.; Wang, C.; Collinson, M. M.; Kundu, S. C.; Yadavalli, V. K. *Biosensors and Bioelectronics* **2016**, 81, 294-302.
73. Colosi, C.; Shin, S. R.; Manoharan, V.; Massa, S.; Costantini, M.; Barbetta, A.; Dokmeci, M. R.; Dentini, M.; Khademhosseini, A. *Advanced Materials* **2016**, 28, 677-684.
74. Kolesky, D. B.; Truby, R. L.; Gladman, A. S.; Busbee, T. A.; Homan, K. A.; Lewis, J. A. *Advanced materials* **2014**, 26, 3124-3130.
75. Du, M.; Chen, B.; Meng, Q.; Liu, S.; Zheng, X.; Zhang, C.; Wang, H.; Li, H.; Wang, N.; Dai, J. *Biofabrication* **2015**, 7, 044104.
76. Radhakumary, C.; Antonty, M.; Sreenivasan, K. *Carbohydrate polymers* **2011**, 83, 705-713.
77. Tran, N. Q.; Joung, Y. K.; Lih, E.; Park, K. D. *Biomacromolecules* **2011**, 12, 2872-2880.

78. Konieczynska, M. D.; Villa-Camacho, J. C.; Ghobril, C.; Perez-Viloria, M.; Tevis, K. M.; Blessing, W. A.; Nazarian, A.; Rodriguez, E. K.; Grinstaff, M. W. *Angewandte Chemie International Edition* **2016**, 55, 9984-9987.
79. Voigt, J.; Driver, V. R. *Wound Repair and Regeneration* **2012**, 20, 317-331.
80. Dahlgren, L. A.; Milton, S. C.; Boswell, S. G.; Werre, S. R.; Brewster, C. C.; Jones, C. S.; Crisman, M. V. *Journal of Equine Veterinary Science* **2016**, 44, 90-99.
81. Bourguignon, L. Y.; Ramez, M.; Gilad, E.; Singleton, P. A.; Man, M.-Q.; Crumrine, D. A.; Elias, P. M.; Feingold, K. R. *Journal of Investigative Dermatology* **2006**, 126, 1356-1365.
82. David-Raoudi, M.; Tranchepain, F.; Deschrevel, B.; Vincent, J. C.; Bogdanowicz, P.; Boumediene, K.; Pujol, J. P. *Wound Repair and Regeneration* **2008**, 16, 274-287.
83. Gao, F.; Liu, Y.; He, Y.; Yang, C.; Wang, Y.; Shi, X.; Wei, G. *Matrix biology* **2010**, 29, 107-116.
84. Bullard, K. M.; Longaker, M. T.; Lorenz, H. P. *World journal of surgery* **2003**, 27, 54-61.
85. Kirker, K. R.; Luo Y.; Shelby, J. H.; Nielson, J.; Prestwich, G. D. **2002**, *Biomaterials*, 23, 3661-3671.
86. Tokatlian,T.; Cam, C.; Segura, T. **2015**, *Adv. Healthcare Mater*., 4, 1084-1091.
87. Burg, K. J.; Porter, S.; Kellam, J. F. *Biomaterials* **2000**, 21, 2347-2359.
88. Pina, S.; Oliveira, J. M.; Reis, R. L. *Advanced Materials* **2015**, 27, 1143-1169.
89. Docherty-Skogh, A.-C.; Bergman, K.; Waern, M. J.; Ekman, S.; Hultenby, K.; Ossipov, D.; Hilborn, J.; Bowden, T.; Engstrand, T. *Plastic and reconstructive surgery* **2010**, 125, 1383-1392.
90. Ni, P.; Ding, Q.; Fan, M.; Liao, J.; Qian, Z.; Luo, J.; Li, X.; Luo, F.; Yang, Z.; Wei, Y. *Biomaterials* **2014**, 35, 236-248.
91. Vashist, A.; Vashist, A.; Gupta, Y.; Ahmad, S. *Journal of Materials Chemistry B* **2014**, 2, 147-166.
92. Norouzi, M.; Nazari, B.; Miller, D. W. *Drug discovery today* **2016**, 21, 1835-1849.

Acta Universitatis Upsaliensis

Digital Comprehensive Summaries of Uppsala Dissertations from the Faculty of Science and Technology 1690

Editor: The Dean of the Faculty of Science and Technology

A doctoral dissertation from the Faculty of Science and Technology, Uppsala University, is usually a summary of a number of papers. A few copies of the complete dissertation are kept at major Swedish research libraries, while the summary alone is distributed internationally through the series Digital Comprehensive Summaries of Uppsala Dissertations from the Faculty of Science and Technology. (Prior to January, 2005, the series was published under the title "Comprehensive Summaries of Uppsala Dissertations from the Faculty of Science and Technology".)

Distribution: publications.uu.se
urn:nbn:se:uu:diva-355252

ACTA
UNIVERSITATIS
UPSALIENSIS
UPPSALA
2018